Candi E, Terrinoni A, Rufini A, Chikh A, Lena AM, Suzuki Y *et al.* (2006). p63 is upstream of IKK alpha in epidermal development. *J Cell Sci* **119**: 4617–4622.

Chiba T, Kita K, Zheng YW, Yokosuka O, Saisho H, Iwama A *et al.* (2006). Side population purified from hepatocellular carcinoma cells harbors cancer stem cell-like properties. *Hepatology* **44**: 240–251.

Eckerdt F, Strebhardt K. (2006). Polo-like kinase 1: target and regulator of anaphase-promoting complex/cyclosome-dependent proteolysis. *Cancer Res* **66**: 6895–6898.

Flores ER, Tsai KY, Crowley D, Sengupta S, Yang A, McKeon F *et al.* (2002). p63 and p73 are required for p53-dependent apoptosis in response to DNA damage. *Nature* **416**: 560–564.

Ghioni P, D'Alessandra Y, Mansueto G, Jaffray E, Hay RT, La Mantia G *et al.* (2005). The protein stability and transcriptional activity of p63alpha are regulated by SUMO-1 conjugation. *Cell Cycle* **4**: 183–190.

Gressner O, Schilling T, Lorenz K, Schulze Schleithoff E, Koch A, Schulze-Bergkamen H *et al.* (2005). TAp63alpha induces apoptosis by activating signaling via death receptors and mitochondria. *EMBO J* **24**: 2458–2471.

Huang YP, Wu G, Guo Z, Osada M, Fomenkov T, Park HL *et al.* (2004). Altered sumoylation of p63alpha contributes to the split-hand/foot malformation phenotype. *Cell Cycle* **3**: 1587–1596.

Ichikawa T, Suenaga Y, Koda T, Ozaki T, Nakagawara A. (2008). TAp63-dependent induction of growth differentiation factor 15 (GDF15) plays a critical role in the regulation of keratinocyte differentiation. *Oncogene* **27**: 409–420.

Kato S, Shimada A, Osada M, Ikawa S, Obinata M, Nakagawara A *et al.* (1999). Effects of p51/p63 missense mutations on transcriptional activities of p53 downstream gene promoters. *Cancer Res* **59**: 5908–5911.

Koga F, Kawakami S, Fujii Y, Saito K, Ohtsuka Y, Iwai A *et al.* (2003). Impaired p63 expression associates with poor prognosis and uroplakin III expression in invasive urothelial carcinoma of the bladder. *Clin Cancer Res* **9**: 5501–5507.

Koida N, Ozaki T, Yamamoto H, Ono S, Koda T, Ando K *et al.* (2008). Inhibitory role of Plk1 in the regulation of p73-dependent apoptosis through physical interaction and phosphorylation. *J Biol Chem* **283**: 8555–8563.

Koster MI, Kim S, Mills AA, DeMayo FJ, Roop DR. (2004). p63 is the molecular switch for initiation of an epithelial stratification program. *Genes Dev* **18**: 126–131.

Levine AJ. (1997). p53, the cellular gatekeeper for growth and division. *Cell* **88**: 323–331.

Lu LY, Wood JL, Minter-Dykhouse K, Ye L, Saunders TL, Yu X *et al.* (2008). Polo-like kinase 1 is essential for early embryonic development and tumor suppression. *Mol Cell Biol* **28**: 6870–6876.

MacPartlin M, Zeng SX, Lu H. (2008). Phosphorylation and stabilization of TAp63gamma by IkappaB kinase-beta. *J Biol Chem* **283**: 15754–15761.

Massion PP, Taflan PM, Jamshedur Rahman SM, Yildiz P, Shyr Y, Edgerton ME *et al.* (2003). Significance of p63 amplification and overexpression in lung cancer development and prognosis. *Cancer Res* **63**: 7113–7121.

Mills AA, Zheng B, Wang XJ, Vogel H, Roop DR, Bradley A. (1999). p63 is a p53 homologue required for limb and epidermal morphogenesis. *Nature* **398**: 708–713.

Moll UM, Slade N. (2004). p63 and p73: roles in development and tumor formation. *Mol Cancer Res* **2**: 371–386.

Montesano R, Hainaut P, Wild CP. (1997). Hepatocellular carcinoma: from gene to public health. *J Natl Cancer Inst* **89**: 1844–1851.

Nakajima H, Toyoshima-Morimoto F, Taniguchi E, Nishida E. (2003). Identification of a consensus motif for Plk (Polo-like kinase) phosphorylation reveals Myt1 as a Plk1 substrate. *J Biol Chem* **278**: 25277–25280.

Nguyen BC, Lefort K, Mandinova A, Antonini D, Devgan V, Della Gatta G *et al.* (2006). Cross-regulation between Notch and p63 in keratinocyte commitment to differentiation. *Genes Dev* **20**: 1028–1042.

Parkin DM, Bray F, Ferlay J, Pisani P. (2001). Estimating the world cancer burden: Globocan 2000. *Int J Cancer* **94**: 153–156.

Petitjean A, Cavard C, Shi H, Tribollet V, Hainaut P, Caron de Fromentel C. (2005). The expression of TA and DeltaNp63 are regulated by different mechanisms in liver cells. *Oncogene* **24**: 512–519.

Rocco JW, Leong CO, Kuperwasser N, DeYoung MP, Ellisen LW. (2006). p63 mediates survival in squamous cell carcinoma by suppression of p73-dependent apoptosis. *Cancer Cell* **9**: 45–56.

Sasaki Y, Ishida S, Morimoto I, Yamashita T, Kojima T, Kihara C *et al.* (2002). The p53 family member genes are involved in the Notch signal pathway. *J Biol Chem* **277**: 719–724.

Shen HM, Ong CN. (2004). Mutations of the p53 tumor suppressor gene and ras oncogenes in aflatoxin hepatocarcinogenesis. *Mutat Res* **366**: 23–44.

Shieh SY, Ikeda M, Taya Y, Prives C. (1997). DNA damage-induced phosphorylation of p53 alleviates inhibition by MDM2. *Cell* **91**: 325–334.

Smits VA, Klompmaker R, Arnaud L, Rijksen G, Nigg EA, Medema RH. (2000). Polo-like kinase-1 is a target of the DNA damage checkpoint. *Nat Cell Biol* **2**: 672–676.

Strebhardt K, Ullrich A. (2006). Targeting polo-like kinase 1 for cancer therapy. *Nat Rev Cancer* **6**: 321–330.

Suh EK, Yang A, Kettenbach A, Bamberger C, Michaelis AH, Zhu Z *et al.* (2006). p63 protects the female germ line during meiotic arrest. *Nature* **444**: 624–628.

Urist MJ, Di Como CJ, Lu ML, Charytonowicz E, Verbel D, Crum CP *et al.* (2002). Loss of p63 expression is associated with tumor progression in bladder cancer. *Am J Pathol* **161**: 1199–1206.

van Vugt MA, Smits VA, Klompmaker R, Medema RH. (2001). Inhibition of Polo-like kinase-1 by DNA damage occurs in an ATM- or ATR-dependent fashion. *J Biol Chem* **276**: 41656–41660.

Vousden KH, Lu X. (2002). Live or let die: the cell's response to p53. *Nat Rev Cancer* **2**: 594–604.

Westfall MD, Joyner AS, Barbieri CE, Livingstone M, Pietenpol JA. (2005). Ultraviolet radiation induces phosphorylation and ubiquitin-mediated degradation of DeltaNp63alpha. *Cell Cycle* **4**: 710–716.

Westfall MD, Mays DJ, Sniezek JC, Pietenpol JA. (2003). The Delta Np63 alpha phosphoprotein binds the p21 and 14-3-3 sigma promoters *in vivo* and has transcriptional repressor activity that is reduced by Hay–Wells syndrome-derived mutations. *Mol Cell Biol* **23**: 2264–2276.

Winkles JA, Alberts GF. (2005). Differential regulation of polo-like kinase 1, 2, 3, and 4 gene expression in mammalian cells and tissues. *Oncogene* **24**: 260–266.

Yamada S, Ohira M, Horie H, Ando K, Takayasu H, Suzuki Y *et al.* (2004). Expression profiling and differential screening between hepatoblastomas and the corresponding normal livers: identification of high expression of the PLK1 oncogene as a poor-prognostic indicator of hepatoblastomas. *Oncogene* **23**: 5901–5911.

Yang A, Kaghad M, Wang Y, Gillett E, Fleming MD, Dötsch V *et al.* (1998). p63, a p53 homolog at 3q27-29, encodes multiple products with transactivating, death-inducing, and dominant-negative activities. *Mol Cell* **2**: 305–316.

Yang A, Schweitzer R, Sun D, Kaghad M, Walker N, Bronson RT *et al.* (1999). p63 is essential for regenerative proliferation in limb, craniofacial and epithelial development. *Nature* **398**: 714–718.

Zhou J, Zhang Y. (2008). Cancer stem cells: models, mechanisms and implications for improved treatment. *Cell Cycle* **7**: 1360–1370.

Supplementary Information accompanies the paper on the Oncogene website (http://www.nature.com/onc)

THE JOURNAL OF BIOLOGICAL CHEMISTRY VOL. 284, NO. 48, pp. 33185–33194, November 27, 2009

Reactive Oxygen Species-generating Mitochondrial DNA Mutation Up-regulates Hypoxia-inducible Factor-1α Gene Transcription via Phosphatidylinositol 3-Kinase-Akt/Protein Kinase C/Histone Deacetylase Pathway*[S]

Received for publication, August 13, 2009, and in revised form, September 20, 2009 Published, JBC Papers in Press, October 1, 2009, DOI 10.1074/jbc.M109.054221

Nobuko Koshikawa[‡], Jun-Ichi Hayashi[§], Akira Nakagawara[¶1], and Keizo Takenaga[‡‖2]

From the [‡]Laboratory of Cancer Metastasis and [¶]Division of Biochemistry and Innovative Cancer Therapeutics, Chiba Cancer Center Research Institute, 666-2 Nitona, Chuoh-ku, Chiba 260-8717, the [§]Graduate School of Life and Environmental Sciences, University of Tsukuba, 1-1-1 Tennodai, Tsukuba, Ibaraki 305-8572, and the [‖]Laboratory of Tumor Biology, Division of Life Science, Shimane University Faculty of Medicine, 89-1 Enya, Izumo, Shimane 693-8501, Japan

Lewis lung carcinoma-derived high metastatic A11 cells constitutively overexpress hypoxia-inducible factor (HIF)-1α mRNA compared with low metastatic P29 cells. Because A11 cells exclusively possess a G13997A mutation in the mitochondrial NADH dehydrogenase subunit 6 (*ND6*) gene, we addressed here a causal relationship between the *ND6* mutation and the activation of *HIF-1α* transcription, and we investigated the potential mechanism. Using trans-mitochondrial cybrids between A11 and P29 cells, we found that the *ND6* mutation was directly involved in *HIF-1α* mRNA overexpression. Stimulation of *HIF-1α* transcription by the *ND6* mutation was mediated by overproduction of reactive oxygen species (ROS) and subsequent activation of phosphatidylinositol 3-kinase (PI3K)-Akt and protein kinase C (PKC) signaling pathways. The up-regulation of *HIF-1α* transcription was abolished by mithramycin A, an Sp1 inhibitor, but luciferase reporter and chromatin immunoprecipitation assays indicated that Sp1 was necessary but not sufficient for *HIF-1α* mRNA overexpression in A11 cells. On the other hand, trichostatin A, a histone deacetylase (HDAC) inhibitor, markedly suppressed *HIF-1α* transcription in A11 cells. In accordance with this, HDAC activity was high in A11 cells but low in P29 cells and in A11 cells treated with the ROS scavenger ebselene, the PI3K inhibitor LY294002, and the PKC inhibitor Ro31-8220. These results suggest that the ROS-generating *ND6* mutation increases *HIF-1α* transcription via the PI3K-Akt/PKC/HDAC pathway, leading to HIF-1α protein accumulation in hypoxic tumor cells.

Somatic mutations in mitochondrial DNA (mtDNA) have been shown to accumulate in cancer cells and proposed to contribute to the progression of cancers of a variety of tissue origins. Mitochondria are the key regulators of the oxidative phosphorylation system that is composed of five complexes (I–V). Some somatic mtDNA mutations are envisioned as inhibiting the electron transport chain, resulting in a marked increase in mitochondrial reactive oxygen species (ROS)[3] production (1). Actually, for example, a heteroplasmic frameshift mtDNA mutation in the NADH dehydrogenase subunit 5 (*ND5*) gene and a deletion mutant of cytochrome B (*CYTB*) gene promote ROS generation (2, 3). In addition, we have recently reported that a missense mutation in the *ND6* gene causes the reduction of complex I activity, ROS overproduction, and increased metastatic potential of Lewis lung carcinoma cells (4).

Hypoxia is a common characteristic of locally advanced solid tumors. Hypoxic tumor cells activate many genes, including those related to cell survival, glycolysis, and angiogenesis, and invasion and metastasis to adapt to and escape from the microenvironment (5, 6). The oxygen-sensing mechanisms have been studied extensively and revealed hypoxia-inducible factors (HIFs) as the key regulatory transcription factors that are composed of HIF-α subunit and HIF-β/ARNT subunit. Under normoxic conditions, the α subunit (HIF-1α) is hydroxylated at Pro^{564} and Pro^{402} by specific Fe^{2+}, oxoglutarate, and oxygen-dependent prolyl hydroxylases, recognized and ubiquitinated by an E3 ubiquitin ligase complex consisting of the tumor suppressor VHL (von Hippel-Lindau), elongin B and elongin C, and rapidly degraded through the ubiquitin-proteasome pathway, whereas the β subunit of HIF-1 (HIF-1β) is constitutively expressed. Under hypoxic conditions, HIF-1α protein is stabilized, allowing its nuclear translocation and dimerization with HIF-1β. In the nucleus, HIF binds to the hypoxia response element of hypoxia-inducible genes, including vascular endothe-

* This work was supported in part by Grants-in-aid for Third Term Comprehensive Control Research for Cancer from the Ministry of Health, Labor, and Welfare (to K. T.) and by Grants-in-aid for Scientific Research from the Ministry of Education, Culture, Sports, Science, and Technology of Japan (to N. K. and K. T.).

[S] The on-line version of this article (available at http://www.jbc.org) contains supplemental Figs. S1–S3 and Table S1.

[1] To whom correspondence may be addressed: 666-2 Nitona, Chuoh-ku, Chiba 260-8717, Japan. Fax: 81 43 265 4459; E-mail: akiranak@chiba-cc.jp.

[2] To whom correspondence may be addressed: 89-1 Enya, Izumo, Shimane 693-8501, Japan. Fax: 81 853 20 2340; E-mail: biokeizo@med.shimane-u.ac.jp.

[3] The abbreviations used are: ROS, reactive oxygen species; DCFH-DA, 2′,7′-dichlorofluorescin diacetate; DMEM, Dulbecco's modified Eagle's medium; DPBS, Dulbecco's phosphate-buffered saline; EMSA, electrophoretic mobility shift assay; ERK, extracellular signal-regulated kinase; FACS, fluorescence-activated cell sorter; HDAC, histone deacetylase; HIF-1α, hypoxia-inducible factor-1α; JNK, c-Jun N-terminal kinase; MAP, mitogen-activated protein; ND6, NADH dehydrogenase subunit 6; PDTC, pyrrolidine dithiocarbamate; PI3K, phosphatidylinositol 3-kinase; PKC, protein kinase C; PMSF, phenylmethylsulfonyl fluoride; TSA, trichostatin A; VEGF, vascular endothelial growth factor.

lial growth factor (VEGF), and transactivates their transcription (5, 6).

Elevated HIF-1α protein levels are commonly observed in many tumor tissues and associated with increased angiogenesis, resistance to apoptosis and chemo- and radiotherapy, and poor patient prognosis (6, 7). Hypoxia generated by aberrant vasculature formation and high interstitial pressure is undoubtedly a major factor, but other factors such as activation of *HIF-1α* gene transcription may also play a role in up-regulation of HIF-1α protein in tumor tissues. Actually, we and others have reported the up-regulation of *HIF-1α* mRNA in some tumor types (8–10). Although the precise mechanism of *HIF-1α* gene activation is largely unknown, an increase in gene dosage is reported as one of the mechanisms of constitutive up-regulation of *HIF-1α* mRNA expression (9, 10).

ROS are the physiological mediators to stabilize and increase the transcriptional activity of HIF-1α protein. Incubation of cells with H_2O_2 or an oxidative stressor leads to the stabilization of HIF-1α protein and activation of HIF target genes under normoxic conditions (11). Conversely, treatment of cells with antioxidants such as *N*-acetylcysteine and glutathione attenuates HIF-1α protein accumulation and the expressions of HIF target genes in various cell types (11). HIF-1α protein levels increase under normoxia in response to growth factors, hormones, coagulation factors, cytokines, and vasoactive peptides, which also stimulate ROS generation (12, 13). Mitochondria-derived ROS produced by electron transport chain complex III are also reported to be able to stabilize HIF-1α protein under hypoxic conditions (14). Although the stabilization of HIF-1α protein by ROS has been highlighted, *HIF-1α* mRNA expression is also stimulated by ROS from NADPH oxidase (15).

So far, there are no reports of the involvement of mtDNA mutations in the activation of the *HIF-1α* gene. Given a high frequency of mtDNA mutation rate in tumor cells and ROS-mediated HIF-1α accumulation at both the protein and mRNA levels, we reasoned that mtDNA mutations could be a cause of *HIF-1α* transcriptional activation. In the present study, we addressed this issue and investigated the potential mechanism. We report here that certain ROS-generating mtDNA mutations can stimulate *HIF-1α* transcription via the phosphatidylinositol 3-kinase (PI3K)/protein kinase C (PKC)/histone deacetylase (HDAC) pathway.

EXPERIMENTAL PROCEDURES

Reagents—Actinomycin D was purchased from Sigma-Aldrich; and SB203580, LY294002, Ro31-8220, ebselene, pyrrolidine dithiocarbamate (PDTC), trichostatin A (TSA), mithramycin A, sulfasarazine, and curcumin were from Calbiochem. SP600125 was obtained from TOCRIS Cookson, Ellisville, MO, and PD98059 was from Cell Signaling Technology, Beverly, MA.

Antibodies—Monoclonal anti-HIF-1α antibody was obtained from Novus Biologicals, Littleton, CO. Polyclonal anti-p38 MAP kinase, anti-phospho-p38 MAP kinase (Thr^{180}/Tyr^{182}), anti-p44/42 MAP kinase, anti-phospho-p44/42 MAP kinase (Thr^{202}/Tyr^{185}), anti-SAPK/JNK, anti-phospho-SAPK/JNK (Thr^{183}/Tyr^{185}), anti-Akt, and anti-phospho-Akt (Ser^{473}), were purchased from Cell Signaling Technology. Polyclonal anti-Sp1, anti-Sp3, anti-E2F-1 antibodies and normal rabbit IgG were obtained from Santa Cruz Biotechnology, monoclonal anti-β-actin antibody was from Sigma-Aldrich, and polyclonal anti-acetylhistone H4 antibody was from Upstate, Charlottesville, VA.

Cell Lines and Culture Conditions—Low metastatic P29 and P34 cells and high metastatic D6 and A11 cells, all of which were derived from Lewis lung carcinoma, were characterized previously (4, 8, 16). Trans-mitochondrial cybrids were established as described previously (4). P29mtA11 cybrids carry nuclear DNA from P29 cells and mtDNA from A11 cells, and A11mtP29 cybrids carry nuclear DNA from A11 cells and mtDNA from P29 cells. As controls, P29mtP29 cybrids, which have nuclear DNA from P29 cells and mtDNA from P29 cells, and A11mtA11 cybrids, which have nuclear DNA from A11 cells and mtDNA from A11 cells, were used. Lewis lung carcinoma cells were maintained in Dulbecco's modified Eagle's medium (DMEM) supplemented with heat-inactivated (56 °C, 30 min) fetal bovine serum, 100 units/ml penicillin, and 100 μg/ml streptomycin. Trans-mitochondrial cybrids were maintained in DMEM supplemented with heat-inactivated fetal bovine serum, 100 units/ml penicillin, 100 μg/ml streptomycin, 0.01% pyruvate, and 0.005% uridine. For hypoxic culture, they were incubated under hypoxic conditions (1% O_2) in a NAPCO® automatic O_2/CO_2 incubator (Precision Scientific, Chicago, IL).

Sequencing of the ND6 Gene—Total DNAs extracted from P29, P34, D6, and A11 cells were used for amplification of the *ND6* gene. The primers used for PCRs were as follows: the forward primer (n.p. 14,030 to 14,053, 5′-CAATTTCACAGCACCAAATCTCCA-3′) and the reverse primer (n.p. 14,759 to 14,779, 5′-TATTAGGGGGTTAGTTTTGCG-3′). All PCR amplifications were performed in a 50 μl of solution consisting of 1× PCR buffer, 0.2 mM dinucleotide triphosphates, 0.6 μM primers, 1 unit of *ExTaq* DNA polymerase (TaKaRa BIO, Shiga, Japan), and 10 ng of genomic DNA as a template. Reaction conditions were 94 °C for 1 min with cycle times of 30 s for denaturation at 94 °C, 30 s for annealing at 53 °C, and 1 min for extension at 72 °C for 30 cycles. The final extension was for 1 min. Amplified *ND6* fragments were separated on 1% agarose gels and extracted and then directly sequenced using a Big Dye Terminator version 3.1 cycle sequencing kit (Applied Biosystems).

Measurement and Visualization of ROS Generation—ROS generation was detected with 2′,7′-dichlorofluorescin diacetate (DCFH-DA) (Molecular Probes, Eugene, OR). Briefly, the cells cultured in 35-mm-diameter glass-bottom culture dishes (MatTeck, Ashland, MA) were incubated with 10 μM DCFH-DA for 10 min at 37 °C in serum-free DMEM, washed twice with Dulbecco's phosphate-buffered saline (DPBS), and then immediately observed under a confocal laser microscope (Fluoview; Olympus, Tokyo) or analyzed with a FACScan flow cytometer (Beckton Dickinson). Mean fluorescence intensity was analyzed using CellQuest software (Becton Dickinson).

RNA Isolation and Northern Blotting—Total RNA was extracted with guanidinium thiocyanate. Total RNA (20 μg) was electrophoresed on 1% agarose gels containing formaldehyde and transferred onto nylon filters. Blots were hybridized

with a ^{32}P-labeled mouse *HIF-1α* cDNA probe or a mouse *VEGF* cDNA probe (8), which was prepared by the random primer method. Filters were finally washed at 50 °C in 30 mM NaCl, 3 mM sodium citrate, and 0.1% SDS.

SDS-PAGE and Western Blotting—Total cell lysates were prepared by directly solubilizing cells in SDS sample buffer. For analyzes of phosphorylated proteins, cells were lysed in 1% Nonidet P-40, 150 mM NaCl, 10% glycerol, 2 mM EDTA, 20 mM Tris-HCl (pH 8.0), 1 mM dithiothreitol, 1 mM Na_3VO_4, 1 mM phenylmethylsulfonyl fluoride (PMSF), and protease inhibitor mixture (Roche Applied Science). Nuclear extracts were prepared using a nuclear extraction kit (Active Motif, Carlsbad, CA) according to the manufacturer's protocol. Proteins were resolved by SDS-PAGE under reducing conditions. Protein concentration was determined by the method of Bradford using bovine serum albumin as a standard. The resolved proteins were transferred electrophoretically to nitrocellulose membrane. After incubating with 5% dry milk in TBS-T (150 mM NaCl, 50 mM Tris-HCl (pH 7.4), 0.05% Tween 20) for at least 1 h at room temperature, the membrane was incubated with polyclonal or monoclonal antibody for the appropriate time, washed extensively with TBS-T, and then incubated with horseradish peroxidase-conjugated goat anti-rabbit or anti-mouse IgG, respectively. Proteins were detected using ECL Western blotting detection reagents (Amersham Biosciences).

Luciferase Reporter Plasmid Construction—Murine *HIF-1α* promoter from nucleotide −1958 to +93 (the transcriptional start site was defined as +1) inserted in the KpnI/SacI site of a luciferase reporter plasmid pGL2-basic, hereafter termed pGL2-HIFpro(−1958/+93), was a generous gift of Dr. C. A. Bradfield, University of Wisconsin Medical School (17). Various truncated forms of the promoter were made by utilizing restriction enzyme recognition sites in the promoter and the vector (XbaI, KpnI/BbrPI, and SacII for making pGL2-HIFpro(−1422/+93), pGL2-HIFpro(−293/+93), and pGL2-HIFpro(−150/+93), respectively) or by PCR using the 5′ primers carrying the KpnI site at the 5′ end and the 3′ primer carrying SacI site at the 3′ end, 5′-GGGAGCTCCGGCTCGGGTTC-3′. The 5′ primers are: 5′-GAGGTACCTCAAGGTCTGTAGGTTGA-3′ for pGL2-HIFpro (−1048/+93), 5′-GAGGTACCATAGCAAAGAGCGGAGAC-3′ for pGL2-HIFpro(−668/+93), 5′-GAGGTACCTTTCCCTCCCCTCGCCGC-3′ for pGL2-HIFpro(−101/+93), and 5′-GAGGTACCCTTCAGCGCCTCAGTGCA-3′ for pGL2-HIFpro(−38/+93). The amplified PCR products were inserted into the KpnI/SacI site of a pGL2-basic vector. A pGL2-HIFpro(−150/+93)mutSp1 plasmid that harbors a mutation in the putative Sp1 binding site was generated by using the QuikChange Site-directed Mutagenesis kit (Stratagene, La Jolla, CA). The sense and the antisense primers used were 5′-CGCCCTTGCCCGAACCCTGCCGCTGC-3′ and 5′-GCAGCGGCAGGGTTCGGGCAAGGGCG-3′, respectively.

Luciferase Reporter Assay—Transient transfection of the luciferase reporter constructs harboring the *HIF-1α* promoter sequence was carried out using Lipofectamine Plus (Invitrogen). As a control for transfection efficiency, pRL-TK vector (Promega, Madison, WI) was cotransfected with test plasmids. pGL2-control vector (Promega) was used as a positive control. Luciferase activity in cell extracts was assayed 45 h after transfection according to the Dual-Luciferase reporter assay system protocols (Promega) using a luminometer (model TD-20/20; Turner Designs, Sunnyvale, CA).

Electrophoretic Mobility Shift Assay (EMSA)—The nuclear protein fractions for EMSA were prepared as described above. Consensus Sp1 (wtSp1, 5′-ATTCGATCGG**GG**CGGGGCGAGC-3′) and mutant Sp1 (mutSp1, 5′-ATTCGATCG**TT**CGGGGCGAGC-3′) double-stranded oligonucleotides were purchased from Santa Cruz Biotechnology. The *HIF-1α* gene promoter-specific double-stranded oligonucleotide probe (positions −72 to −48) (wtHIFpro-Sp1) or its mutant form (mutHIFpro-Sp1) was prepared by annealing the sense 5′-CGCCTCCGCCCTTGCCCG**CC**CCCTG-3′ and the antisense 5′-CAGGGG**GG**CGGGCAAGGGCGGAGGCG-3′ oligonucleotides or the sense 5′-CGCCTCCGCCCTTGCCCG**AA**CCCTG-3′ and the antisense 5′-CAGGG**TT**CGGGCAAGGGCGGAGGCG-3′, respectively. The probes were labeled using [γ-^{32}P]ATP (Amersham Biosciences) and MEGALABEL™ kit (TaKaRa BIO). Five micrograms of nuclear protein, ^{32}P-labeled double-stranded probe (5000 cpm), 1 μg of poly(dI·dC), and 17 μl of binding buffer (20 mM Hepes (pH 7.9), 50 mM NaCl, 5% glycerol, 0.1 mM dithiothreitol) were mixed in a total volume of 20 μl. In competition assays, a 50-fold molar excess amount of unlabeled competitors was included in the reaction mixture. The mixture was incubated at room temperature for 30 min, then loaded on a 5% polyacrylamide gel in TGE buffer (50 mM Tris-HCl (pH 8.5), 380 mM glycine, 2 mM EDTA), and subjected to electrophoresis at 4 °C. The gel was dried and exposed to x-ray film at −70 °C. A supershift assay was performed using 10 μg of specific goat polyclonal anti-Sp1 or anti-Sp3 antibody.

Chromatin Immunoprecipitation Assay—Cells were fixed with 1% formaldehyde for 10 min at 37 °C, and the reaction was quenched by adding glycine to a final concentration of 125 mM. The cells were washed with DPBS containing 1 mM PMSF; centrifuged; swelled in 5 mM Hepes (pH 8.0), 85 mM KCl, 0.5% Nonidet P-40, 0.5 mM PMSF, 100 ng/ml leupeptin, 100 ng/ml aprotinin; incubated for 10 min on ice; and then lysed with a Dounce homogenizer. Nuclei were collected by centrifugation and resuspended in sonication buffer (1% SDS, 10 mM EDTA, 50 mM Tris-HCl (pH 8.0), 0.5 mM PMSF, 100 ng/ml leupeptin, 100 ng/ml aprotinin). The nuclei were sonicated on ice to an average length of 500 to 1000 bp and then centrifuged at 10,000 × *g* for 15 min at 4 °C. The chromatin solution was diluted 10-fold in chromatin immunoprecipitation dilution buffer (500 mM Tris-HCl (pH 8.0), 1670 mM NaCl, 11% Triton X-100, 1.1% sodium deoxycholate, 10 mM PMSF, 10 μg/ml leupeptin, 10 μg/ml aprotinin, 10 μg/ml pepstatin), precleared by the addition of protein A-Sepharose beads for 1 h at 4 °C. Precleared chromatin solution was incubated with 5 μg of anti-Sp1 antibody, anti-Sp3 antibody, or anti-acetylhistone H4 antibodies at 4 °C for 13 h. Normal rabbit IgG served as a control. Protein·DNA complexes were immunoprecipitated by protein A beads, and the cross-links were reversed by heating to 65 °C for 5 h. The DNA was recovered by phenol:chloroform extraction and precipitated by ethanol. Then, the association of Sp1, Sp3, and acetylated histone H4 with the Sp1/Sp3 recognition site in the *HIF-1α* promoter was examined by hot-start PCR

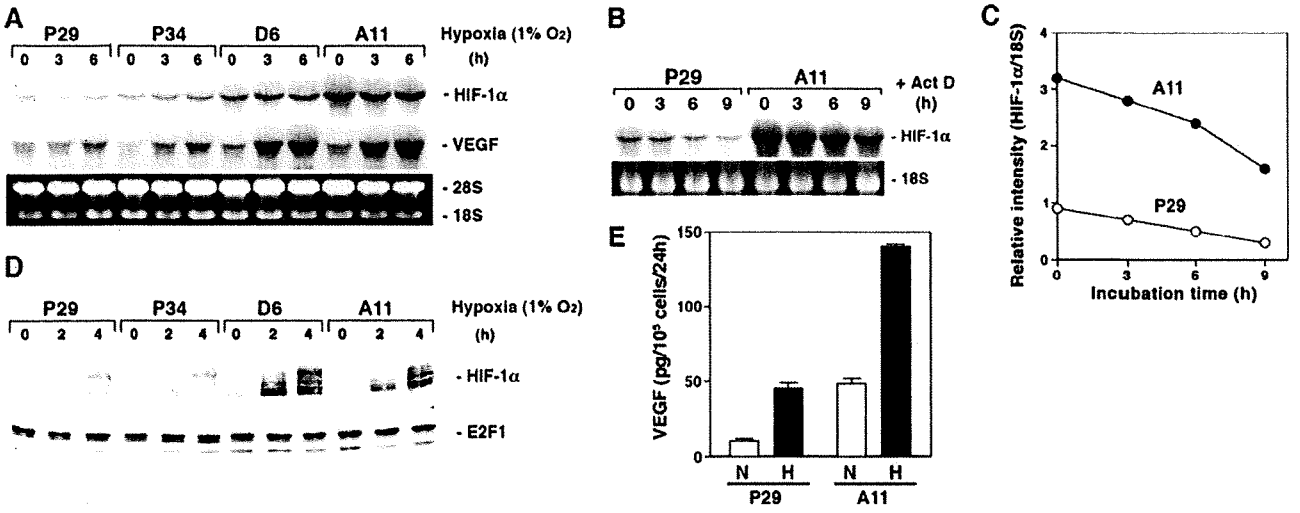

FIGURE 1. **HIF-1α and VEGF expressions are higher in high metastatic D6 and A11 cells than in low metastatic P29 and P34 cells.** *A*, P29, P34, D6, and A11 cells were cultured under hypoxic conditions (1% O_2) for up to 6 h. Total RNA was extracted and subjected to Northern blot analysis. The blots were hybridized with either a ^{32}P-labeled *HIF-1α* or *VEGF* cDNA probe. Ethidium bromide staining of the gel is also shown. *B* and *C*, P29 and A11 cells were incubated with 5 μg/ml actinomycin D (*Act D*) for up to 9 h. Total RNA was extracted and analyzed as above. Ethidium bromide staining of 18 S ribosomal RNA is also shown. After semiquantifying the intensities of bands, the levels of *HIF-1α* mRNA were normalized to those of 18 S ribosomal RNA. *D*, P29, P34, D6, and A11 cells were cultured under hypoxic conditions for up to 4 h. Nuclear extracts prepared from the cells were dissolved by SDS-PAGE. HIF-1α and E2F1, which served as a control, were detected by immunoblotting. *E*, P29 and A11 cells were cultured under normoxic (*N*) or hypoxic (*H*) conditions for 18 h. VEGF produced in the supernatants was measured by enzyme-linked immunosorbent assay. *Bars*, S.D.

using *GoTaq*DNA polymerase (Promega). The sense and the antisense primers used were 5′-ACCTCCTCCTGATTGGCTG-3′ (positions −258 to −239) and 5′-TCGCGTCCCCTCAGCCGA-3′ (positions −12 to +5), respectively. The PCR conditions were: 96 °C for 5 min, 30 cycles with 96 °C for 30 s, 57 °C for 30 s, and 72 °C for 30 s, and 72 °C for 5 min. Final PCR products were analyzed on 2% agarose gels with ethidium bromide staining.

CD31 Staining of Tumor Blood Vessels—P29mtP29, P29mtA11, A11mtA11, and A11mtP29 cells (1×10^6 cells) were inoculated subcutaneously into the abdominal flank of C57BL/6 mice. When an estimated tumor volume reached ~2 cm^3, subcutaneous tumors were surgically removed and immediately frozen in OCT compound. Cryostat sections (10-μm thickness) were made at every 100-μm distance, fixed with 4% paraformaldehyde, and then washed with DPBS. After blocking with 10% normal goat serum in DPBS, sections were incubated with rat anti-mouse CD31 antibody (1:100 dilutions) (BD Pharmingen) overnight at 4 °C. They were washed with DPBS and incubated with fluorescein isothiocyanate-conjugated goat anti-rat IgG. After extensive washing with DPBS, samples were counterstained with 1 μg/ml propidium iodide and observed under a confocal laser microscope (Fluoview). Images were captured and transferred to the ImageJ 1.34s software, and CD31-positive areas were analyzed. In this way, at least six randomly selected fields (0.2 cm^2/field) were analyzed, and the percentage of CD31-positive area per field was calculated.

HDAC Activity Assay—Nuclear extracts were prepared using a nuclear extraction kit. HDAC activity was measured using a HDAC fluorometric assay/drug discovery kit (BioMol International, Plymouth Meeting, PA) according to the manufacturer's instruction. Briefly, 4.5-μg nuclear extracts were incubated with Fluor de Lys substrate buffer at 37 °C for 30 min followed by incubation with Fluor de Lys developer concentrate at 25 °C for 10 min. Fluorescence was measured with a multiwell plate reader (excitation at 355 nm and emission at 460 nm).

RESULTS

Activation of HIF-1α Gene Transcription in High Metastatic Cells—We compared the expression level of *HIF-1α* mRNA between the low metastatic (P29 and P34) and the high metastatic (D6 and A11) cells originated from Lewis lung carcinoma. The results showed that D6 and A11 cells expressed a larger amount of *HIF-1α* mRNA than P29 and P34 cells (Fig. 1*A*). Hypoxia did not affect the expression level of the mRNA. One of the possible mechanisms of *HIF-1α* mRNA up-regulation in D6 and A11 cells may be the difference in *HIF-1α* mRNA stability in the cells. To test this possibility, we cultured P29 and A11 cells in the presence of actinomycin D for up to 9 h and examined the mRNA level at each time point (Fig. 1*B*). The results showed that the half-life of *HIF-1α* mRNA in A11 cells was nearly equal to that in P29 cells (~8 h) (Fig. 1C). Thus, the transcription of the *HIF-1α* gene was found to be more activated in A11 cells than in P29 cells.

Under normoxic conditions, HIF-1α protein was scarcely detected in both the low and the high metastatic cells. However, upon hypoxic exposure, HIF-1α protein level markedly increased in D6 and A11 cells compared with P29 and P34 cells (Fig. 1*D*). Accordingly, hypoxia enhanced the expression of VEGF in D6 and A11 cells more than in P29 and P34 cells at both the mRNA and protein levels (Fig. 1, *A* and *E*). Thus, the up-regulation of *HIF-1α* mRNA in D6 and A11 cells resulted in overexpression of HIF-1α under hypoxic conditions, leading to VEGF overexpression.

ND6 Mutation Activates HIF-1α Transcription—Sequencing of the *ND6* gene revealed that D6 and A11 cells harbored

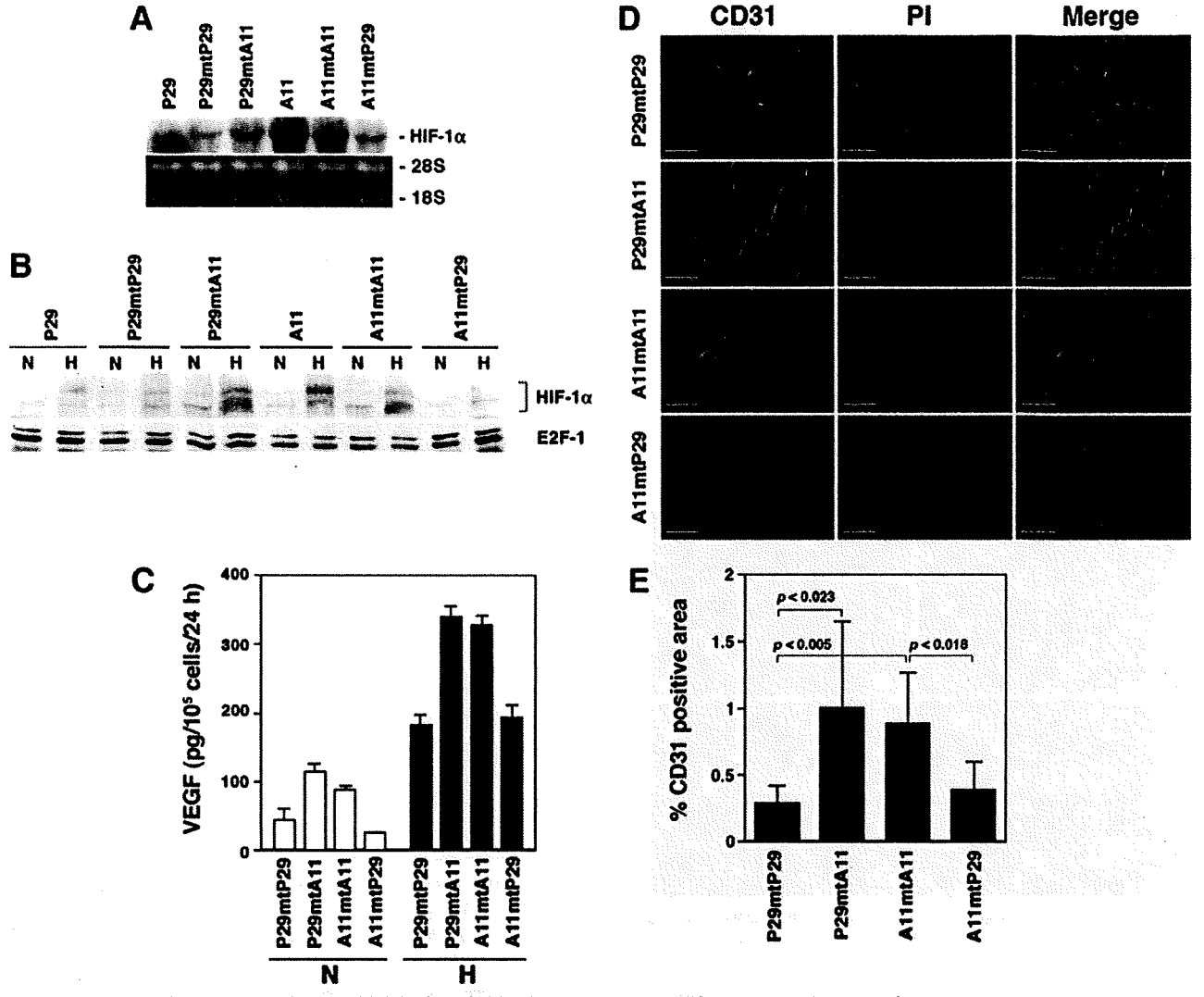

FIGURE 2. **HIF-1α and VEGF expressions are high in the cybrids with mtDNA carrying the *ND6* mutation.** *A*, total RNA extracted from P29, A11, and the cybrids was subjected to Northern blot analysis. The blots were hybridized with a ^{32}P-labeled *HIF-1α* cDNA. Ethidium bromide staining of the gel is also shown. *B*, P29 cells, A11 cells, and the cybrids were cultured under normoxic (*N*) or hypoxic (*H*) conditions for 4 h. Nuclear extracts prepared from the cells were dissolved by SDS-PAGE. HIF-1α and E2F1, which served as a control, were detected by immunoblotting. *C*, the cybrids were cultured under normoxic (*N*) or hypoxic (*H*) conditions for 18 h. VEGF produced in the supernatants was measured by enzyme-linked immunosorbent assay. *Bars*, S.D. *D*, cryostat sections prepared from subcutaneous tumors were stained with anti-CD31 antibody. Sections were counterstained with propidium iodide (*PI*). *E*, blood vessel density in subcutaneous tumors formed by the cybrids was assessed by staining with anti-CD31 antibody. The fluorescent images of at least six fields (0.2 cm^2/field) were analyzed, and the percentage of CD31-positive area/field (*columns*) was calculated. *Bars*, S.D.

a G13997A mutation, which changes evolutionally conserved proline 25 to leucine, whereas P29 and P34 cells did not (Fig. S1 and Table S1). To examine a causal relationship between the *ND6* mutation and *HIF-1α* transcription, we examined *HIF-1α* mRNA levels in trans-mitochondrial cybrids, P29mtA11 and A11mP29 cells, which carry mtDNA from A11 and P29 cells and nuclear DNA from P29 and A11 cells, respectively. We used P29mtP29 and A11mtA11 cells as control cybrids. The results showed that the expression level of *HIF-1α* mRNA was higher in the cybrids with A11 mtDNA (P29mtA11 and A11mtA11) irrespective of whether their nuclear DNA is derived from P29 or A11 cells, than in the cybrids with mtDNA from P29 cells (P29mtP29 and A11mtP29) (Fig. 2*A*). Accordingly, HIF-1α protein and VEGF were highly induced in P29mtA11 and A11mtA11 cybrids under hypoxic conditions compared with A11mtP29 and P29mtP29 cybrids (Fig. 2, *B* and *C*). Furthermore, P29mtA11 and A11mtA11 cybrids showed enhanced angiogenesis *in vivo* (Fig. 2, *D* and *E*). These results indicate that the *HIF-1α* mRNA overexpression in A11 and D6 cells is attributed to the *ND6* mutation.

ROS Are Involved in HIF-1α Transcriptional Activation by the ND6 Mutation—It is possible that mitochondrial ROS production caused by the *ND6* mutation mediates the activation of *HIF-1α* transcription. To examine this possibility, we measured the intracellular ROS level. Fluorescence-activated cell sorter (FACS) analysis and confocal images showed that D6 and A11 cells produced a larger amount of ROS than P29 and P34 cells (Fig. 3). In addition, the cybrids with mtDNA from A11 cells

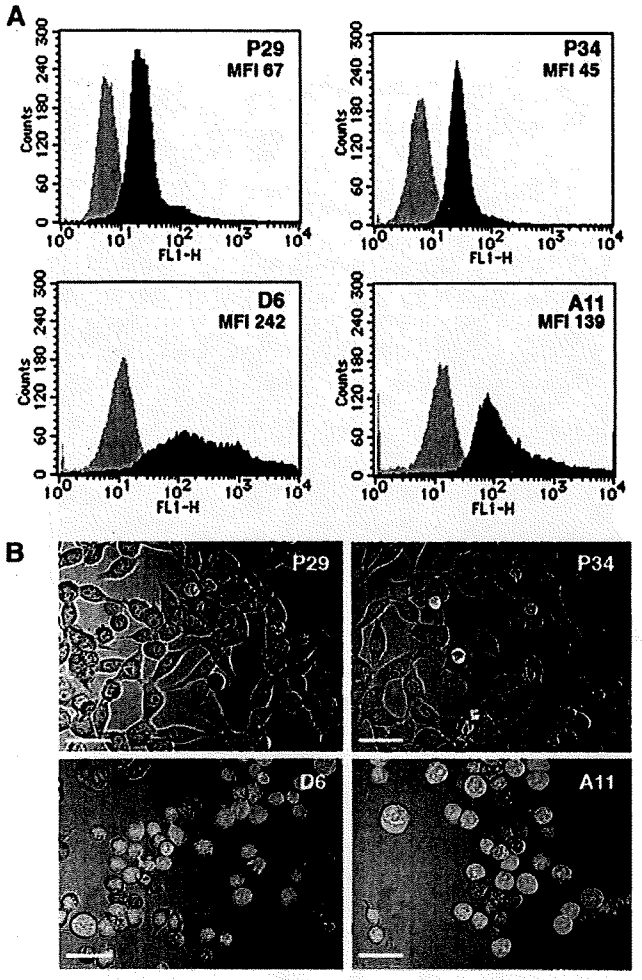

FIGURE 3. **ROS production is elevated in the cells with mtDNA carrying the *ND6* mutation.** *A*, P29, P34, D6, and A11 cells were incubated with 10 μM DCFH-DA for 10 min at 37 °C in serum-free DMEM and then immediately were analyzed with a FACScan flow cytometer. Mean fluorescence intensity (*MFI*) is also shown. *B*, the cells treated as above were observed under a confocal laser microscope.

(P29mtA11 and A11mtA11) overproduced ROS compared with the cybrids with mtDNA from P29 cells (P29mtP29 and A11mtP29) (Fig. S2). Thus, the *ND6* mutation is correlated well with both ROS overproduction and *HIF-1α* mRNA up-regulation.

Next, to gain evidence of a causal relationship between ROS and *HIF-1α* mRNA expression, we examined the effects of general antioxidants ebselene and PDTC, and antimycin A, which inhibits electron transport pathway (18). FACS analysis showed that intracellular ROS level was low in ebselene- and in PDTC-treated cells whereas high in antimycin A-treated cells compared with untreated cells, showing more distinct changes in A11 cells than in P29 cells (Fig. 4*A*). Ebselene and PDTC effectively suppressed the expression of *HIF-1α* mRNA in A11 cells, whereas antimycin A increased the expression in both P29 and A11 cells (Fig. 4*B*). These results strongly suggest that the *HIF-1α* transcriptional activation is regulated by mitochondrial ROS. Supporting this, we found that exogenously added H_2O_2 stimulated the expression of *HIF-1α* mRNA in P29 cells (Fig. 4*C*).

PI3K-Akt and PKC Signaling Pathways Are Involved in Mitochondrial ROS-mediated HIF-1α Overexpression—We next investigated signaling pathways of the mitochondrial ROS-mediated *HIF-1α* gene activation. For this, we treated P29 and A11 cells with PD98059, a MEK1 inhibitor, SB203580, a p38 MAP kinase inhibitor, SP600125, a JNK inhibitor, and LY294002, a PI3K inhibitor. As shown in Fig. 5*A*, LY294002 significantly inhibited *HIF-1α* mRNA expression in A11 cells in a dose-dependent manner, whereas PD98059, SB203580, and SP600125 did not, suggesting the involvement of the PI3K-Akt pathway in the mitochondrial ROS-mediated *HIF-1α* gene transcription. None of these inhibitors significantly suppressed *HIF-1α* mRNA expression in P29 cells, implying that the PI3K-Akt pathway does not contribute to the basal expression level of *HIF-1α* mRNA. In accordance with the data, Akt was highly activated, indicated by its protein phosphorylation, in D6 and A11 cells but not in P29 and P34 cells, and there was no consistent difference in the phosphorylation level of p38 MAP kinase, p44/42 MAP kinase, or JNK (Fig. 5*B*). Akt was also highly activated in P29mtA11 and A11mtA11 cybrids, but not in P29mtP29 and A11mtP29 cybrids (Fig. 5*C*). H_2O_2 strongly induced Akt activation in P29 cells in a time-dependent manner (Fig. 5*D*). Moreover, ebselene inhibited Akt phosphorylation in A11 cells (Fig. 5*E*). Thus, Akt phosphorylation is linked to the level of *HIF-1α* mRNA. In addition, Ro31-8220, a pan-specific PKC inhibitor, markedly inhibited *HIF-1α* mRNA expression in A11 cells, but only slightly in P29 cells, suggesting the involvement of PKC in the ROS-mediated *HIF-1α* mRNA expression (Fig. 5*F*). On the other hand, rapamycin, an mTOR inhibitor, sulfasarazine, an NF-κB inhibitor, and curcumin, an AP-1 inhibitor, did not significantly inhibit *HIF-1α* mRNA expression in A11 cells (Fig. S3). Collectively, these data indicate that the PI3K-Akt and PKC pathways are involved in the ROS-mediated *HIF-1α* transcriptional activation in A11 cells.

Sp1 Is Necessary but Not Sufficient for ROS-mediated HIF-1α Gene Activation—To gain further insight into the underlying mechanisms of *HIF-1α* gene activation in the high metastatic cell lines, we treated the cells with mithramycin A, an Sp1 inhibitor. The results showed that it significantly suppressed the expression of *HIF-1α* mRNA in D6 and A11 cells but not in P29 and P34 cells (Fig. 6*A*), suggesting the involvement of Sp1 in the ROS-mediated *HIF-1α* mRNA overexpression. To examine which region of the *HIF-1α* promoter is responsible for the activated transcription of the gene in A11 cells, we constructed luciferase reporter plasmids harboring the full-length (−1958/+93) and a series of truncated promoters (Fig. 6*B*). We transiently transfected them into A11 cells and examined their activities. The results showed that deletion of the region from −1958 to −101 effectively reduced the promoter activity compared with the full-length promoter, whereas deletion from −1958 to −150 did not significantly reduce the activity. Deletion of the region from −1958 to −38 abrogated the promoter activity, indicating that an important sequence for the promoter activity resides in the region from −149 to −38. Sequence analysis of this region using a computer software (TFSEARCH, Papia system) revealed a putative Sp1 binding

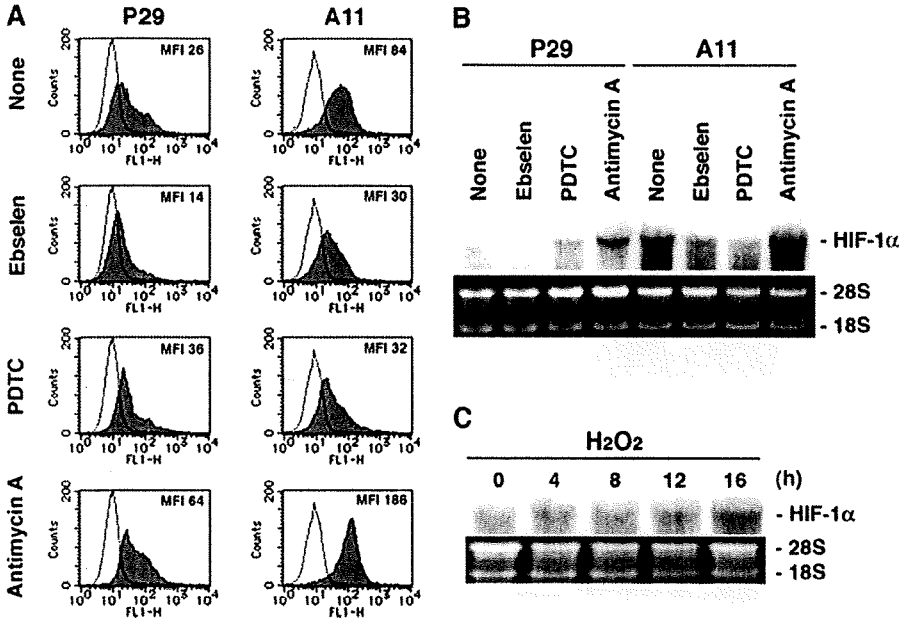

FIGURE 4. **ROS production is correlated with *HIF-1α* mRNA expression.** *A*, P29 and A11 cells were treated with solvent alone (dimethyl sulfoxide) (*None*), ebselen (20 μM), PDTC (20 μg/ml), and antimycin A (20 μg/ml) for 18 h. The cells were incubated with 10 μM DCFH-DA for 10 min at 37 °C in serum-free DMEM and then immediately were analyzed with a FACScan flow cytometer. Mean fluorescence intensity (*MFI*) is also shown. *B*, P29 and A11 cells were treated as above, and total extracted RNA was subjected to Northern blot analysis. The blots were hybridized with ^{32}P-labeled *HIF-1α* cDNA. Ethidium bromide staining of the gel is also shown. *C*, P29 cells were treated with 25 μM H_2O_2 for up to 16 h. Total extracted RNA was analyzed as in *B*.

sequence (−60/−51). Mutation of this sequence TGCCCG-CCCC to TGCCCGAACC significantly reduced the promoter activity (Fig. 6*B*), demonstrating the importance of this sequence for the promoter activity.

To obtain direct evidence that Sp family members bind to this putative Sp1 binding sequence, we carried out EMSAs using wtHIFpro-Sp1 (−72/−48) as a DNA probe. As shown in Fig. 6*C*, these assays revealed three constitutive binding complexes (C1–C3) (*lane 2*) that were almost entirely Sp-dependent, as shown by competition with excess wtHIFpro-Sp1 or Sp1 consensus oligonucleotides (wtSp1) (*lanes 3* and *5*), but not with their mutant form mutHIFpro-Sp1 or mutSp1 (*lanes 4* and *6*). Addition of antibodies directed against either Sp1 or Sp3 induced a supershift and/or a significant reduction of Sp1/Sp3-dependent binding activities (*lanes 7* and *8*). Simultaneous addition of both antibodies led to a nearly complete supershift (*lane 9*). These data indicate that Sp1 and Sp3 proteins actually bind to the region proximal to the transcription initiation site.

We then compared the expression levels of Sp1 and Sp3 between the high and the low metastatic cell lines. However, we could not detect any difference (Fig. 6*D*). Also, the DNA binding activity of Sp1/Sp3, as demonstrated by EMSA analysis, did not correlate with the *HIF-1α* transcriptional level (Fig. 6*E*). Moreover, chromatin immunoprecipitation assays revealed that there were no differences in the binding of Sp1 and Sp3 to the Sp1/Sp3 binding site and the level of histone H4 acetylation around the site between P29 and A11 cells (Fig. 6*F*). These results indicate that Sp1 is necessary but not sufficient for explaining the higher expression of *HIF-1α* mRNA in the high metastatic cell lines.

HDAC Activation Contributes to the ROS-mediated HIF-1α Transcriptional Activation—To investigate a possible mechanism of the *HIF-1α* transcriptional activation in the high metastatic cells further, we treated P29 and A11 cells with TSA, a nonselective HDAC inhibitor. The results showed that TSA dramatically suppressed *HIF-1α* mRNA expression in A11 cells but slightly in P29 cells (Fig. 7*A*), suggesting the relationship between HDAC activity and the ROS-mediated *HIF-1α* mRNA overexpression. Then, we measured HDAC activity in P29 cells, P29 cells treated with H_2O_2, A11 cells, and A11 cells treated with ebselene, antimycin A, LY294002, and Ro31-8220. The results in Fig. 7*B* show that HDAC activity was significantly higher in A11 cells than in P29 cells. It was high in H_2O_2-treated P29 cells and antimycin A-treated A11 cells, but low in A11 cells treated with ebselene, LY294002, and Ro31-8220 compared with the respective untreated cells. Thus, the HDAC activity is positively correlated with the *HIF-1α* mRNA up-regulation.

DISCUSSION

The present study demonstrates that an ROS-generating mtDNA mutation in the *ND6* gene leads to *HIF-1α* mRNA overexpression, resulting in marked up-regulation of HIF-1α protein and VEGF production levels under hypoxic conditions. This study also suggests the possibility for the first time that some of pathogenic mtDNA mutations can activate *HIF-1α* transcription.

mtDNA mutations are frequently observed in tumor cells and implicated to be a factor in the progression of tumors. mtDNA mutations in tumor cells include severe mutations such as insertion-deletion and chain termination mutations and mild missense mutations. The mutation in the *ND6* gene found in A11 cells is a missense mutation that reduces complex I activity (4). This mutation was also found in the other high metastatic D6 cells but not in the low metastatic P29 or P34 cells. In both A11 and D6 cells, up-regulation of *HIF-1α* gene transcription was detected, suggesting a causal linkage between the *ND6* mutation and *HIF-1α* transcription. In the present study, we used trans-mitochondrial cybrids to prove this linkage, and as expected, the cybrids carrying mtDNA from A11 cells overexpressed *HIF-1α* mRNA, despite the source of nuclear DNA.

Several lines of evidence supported that ROS caused by the *ND6* mutation primarily mediates *HIF-1α* transcription. First, the cells carrying A11 mtDNA overproduced ROS. Second, ebselene and PDTC reduced the intracellular ROS level and concomitantly abolished *HIF-1α* transcription. Third, antimy-

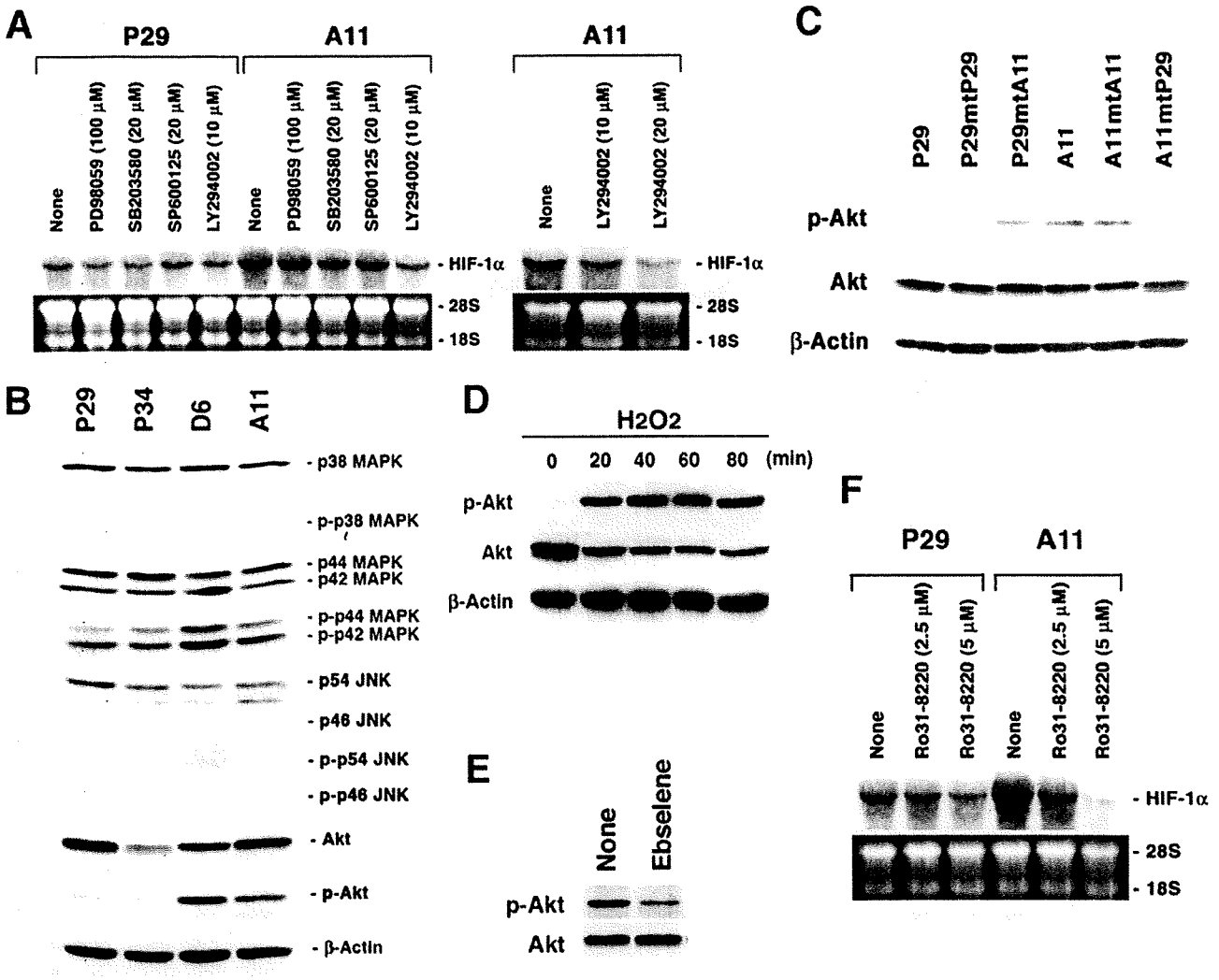

FIGURE 5. **PI3K-Akt and PKC pathways are involved in the ROS-mediated *HIF-1α* mRNA overexpression.** *A*, P29 and A11 cells were treated with dimethyl sulfoxide, PD98059, SB203580, SP600125, and LY294002 at the indicated concentrations for 18 h. Total RNA was extracted and subjected to Northern blot analysis. The blots were hybridized with a ^{32}P-labeled *HIF-1α* cDNA. Ethidium bromide staining of the gel is also shown. *B*, cell lysates prepared from P29, P34, D6, and A11 cells were dissolved by SDS-PAGE. Proteins and phosphorylated proteins and β-actin, which served as a loading control, were detected by immunoblotting. *C*, cell lysates prepared from P29, A11, and the cybrids were subjected to immunoblotting to detect Akt and phosphorylated Akt. β-Actin served as a loading control. *D*, P29 cells were treated with 25 μM H_2O_2 for up to 80 min. Cell lysates were prepared and subjected to immunoblotting as in *C*. *E*, A11 cells were treated with ebselene (20 μM) for 18 h. Cell lysates were prepared and subjected to immunoblotting as in *C*. *F*, P29 and A11 cells were treated with Ro31-8220 at the indicated concentrations for 18 h. Total RNA was analyzed as in *A*.

cin A that inhibits the function of complex III, thereby generating large quantities of superoxide radicals, increased the expression of *HIF-1α* mRNA in both P29 and A11 cells. Fourth, exogenous H_2O_2 enhanced the expression. ROS from NADPH oxidase are also mediators of *HIF-1α* mRNA induction in lipopolysaccharide-stimulated microglial cells and thrombin-stimulated pulmonary artery smooth muscle cells (15, 19). Furthermore, we showed that PI3K-Akt and PKC, but not ERK or JNK, regulate *HIF-1α* mRNA expression. Because both LY29004 and Ro31-8220 suppressed *HIF-1α* mRNA expression more effectively in A11 cells than in P29 cells, PI3K-Akt and PKC may engage in the ROS-mediated expression of *HIF-1α* mRNA. Consistent with these results, either PI3K or PKC or both are shown to regulate *HIF-1α* transcription in lipopolysaccharide-stimulated glial cells, BCR/ABL-expressing Ba/F3 hematopoietic cells, and angiotensin II-treated vascular smooth muscle cells (12, 15, 20). In contrast, ERK and JNK are reported to mediate lipopolysaccharide-stimulated *HIF-1α* mRNA induction in human monocytes/macrophages and hepatoma cells, respectively (21, 22). Further study is required to determine which PKC isoform is responsible for the ROS-mediated expression of *HIF-1α* mRNA using a molecular approach.

The *HIF-1α* gene promoter contains putative binding sites for several transcription factors, including Sp1, AP-1, and NF-κB (23–25). Treatment of A11 cells with mithramycin A resulted in a marked suppression of *HIF-1α* mRNA expression in A11 cells, whereas sulfasarazine and curcumin showed no effect, suggesting the importance of Sp1 for the promoter activity. Luciferase reporter assays also indicated that the Sp1 bind-

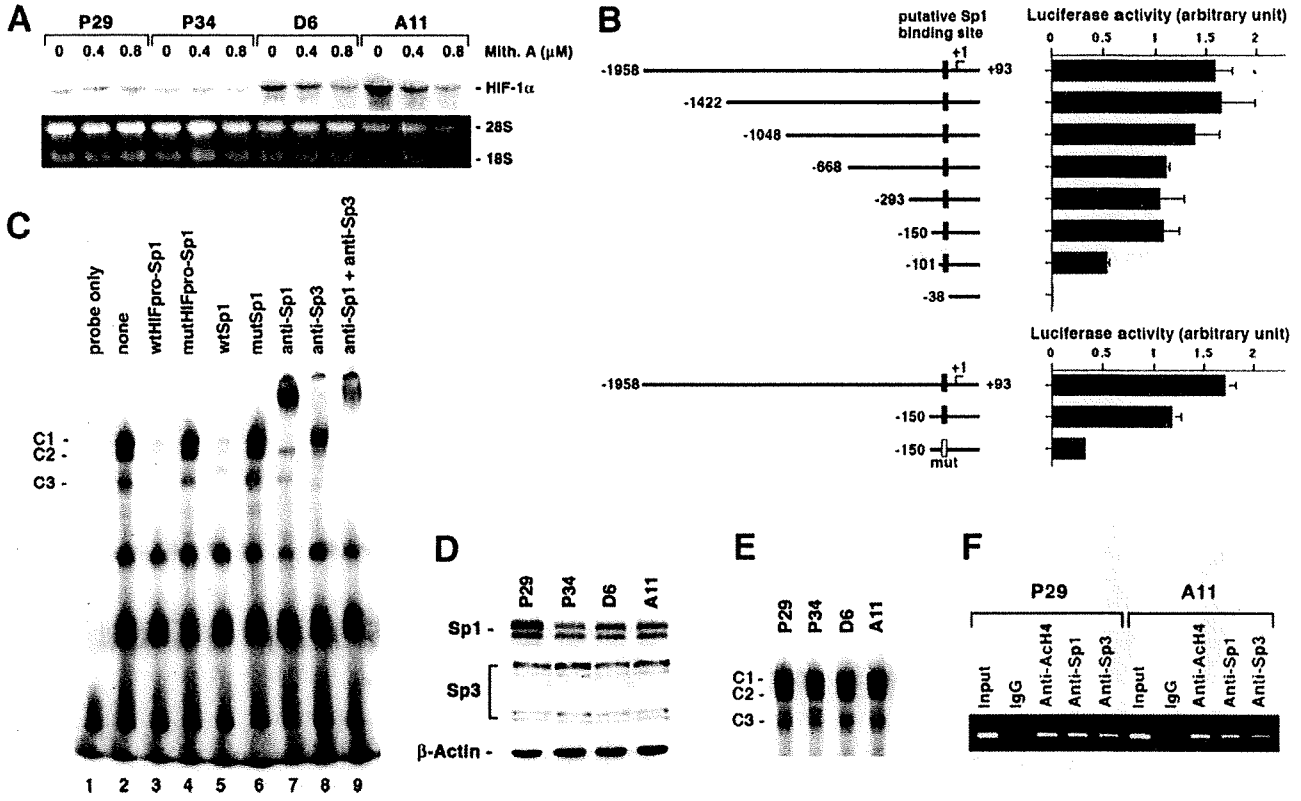

FIGURE 6. **Sp1 is necessary but not sufficient for the ROS-mediated *HIF-1α* mRNA overexpression.** *A*, P29, P34, D6, and A11 cells were treated with mithramycin A at the indicated concentrations for 24 h. Total RNA was extracted and subjected to Northern blot analysis. The blots were hybridized with a ^{32}P-labeled *HIF-1α* cDNA. Ethidium bromide staining of the gel is also shown. *B*, pGL2-basic luciferase reporter plasmids harboring the full-length (−1958/+93) and a series of truncated *HIF-1α* promoters were transfected in A11 cells, and luciferase activity was assayed 45 h after transfection. *Filled* and *open boxes* indicate putative wild-type and mutated Sp1 binding sites, respectively. *C*, nuclear extracts prepared from A11 cells were subjected to EMSAs in which ^{32}P-labeled oligonucleotides (*HIFpro-Sp1*) containing a putative Sp1 binding site was used as a probe. *wtHIFpro-Sp1*, *mutHIFpro-Sp1*, *wtSp1*, and *mutSp1* indicate wild-type HIFpro-Sp1, mutated HIFpro-Sp1, consensus Sp1 and mutated Sp1 oligonucleotides, respectively. *C1–C3* indicate specific Sp-dependent binding complexes. *D*, total cell lysates prepared from P29, P34, D6, and A11 cells were subjected to immunoblotting using anti-Sp1, anti-Sp3 and anti-β-actin antibodies. *E*, nuclear extracts prepared from P29, P34, D6, and A11 cells were subjected to EMSAs as in *C*. *F*, nuclear extracts prepared from P29 and A11 cells were subjected to chromatin immunoprecipitation assays in which anti-acetylated histone H4 (*anti-AcH4*), anti-Sp1, and anti-Sp3 antibodies were used. Normal rabbit IgG served as a control.

ing site is indispensable for the promoter activity. Unexpectedly, however, we could not find any difference in the level of Sp1 binding to and histone acetylation around the binding site between A11 and P29 cells. In contrast, Oh *et al.* (19) reported that lipopolysaccharide induces *HIF-1α* mRNA in an Sp1-dependent pathway. It is necessary to determine whether other regions of the promoter and transcription factors are involved in the overexpression of *HIF-1α* mRNA in A11 cells.

In the present study, we showed that TSA markedly repressed the expression of *HIF-1α* mRNA in A11 cells. Based on this observation, we found a correlation between HDAC activity and *HIF-1α* transcription; that is, HDAC activity was higher in A11 than in P29 cells. It was also higher in H_2O_2-treated P29 cells and antimycin A-treated A11 cells than in the respective control cells. Furthermore, HDAC activity in A11 cells was repressed by ebselene, LY294002, and Ro31-8220. Together, these data indicate that ROS lead to HDAC activation through PI3K and PKC pathways, thereby activating *HIF-1α* transcription. In general, histone acetylation enhances gene expression through the chromatin remodeling caused by histone modification (26). Therefore, it is not clear how HDAC inhibition can lead to the transcriptional repression of the *HIF-1α* gene. However, many genes such as proinflammatory genes, including tumor necrosis factor-α, interleukin-1β, interferon-γ, and inducible nitric-oxide synthase, are reported to be repressed by HDAC inhibitors (27–30). The repression of these proinflammatory genes has been suggested to be a result of inhibition of NF-κB activation and the acetylation of non-histone proteins (30). Because our data indicate little contribution of NF-κB in the ROS-mediated *HIF-1α* mRNA overexpression in A11 cells, acetylation of other non-histone proteins may be important. It should be noted that Noh *et al.* (31) have recently shown that TSA decreases mRNA of extracellular matrix components. They also show that HDAC2 plays an important role in the development of extracellular matrix accumulation and that ROS mediate transforming growth factor-β1-induced activation of HDAC2 (31). HDACs constitute a family of 18 enzymes (32). Therefore, it will be interesting to determine which HDAC is responsible for the ROS-mediated *HIF-1α* transcription in the cells carrying mtDNA with the *ND6* mutation.

In conclusion, our findings show that the ROS-generating *ND6* mutation causes *HIF-1α* transcription via PI3K-Akt/PKC/

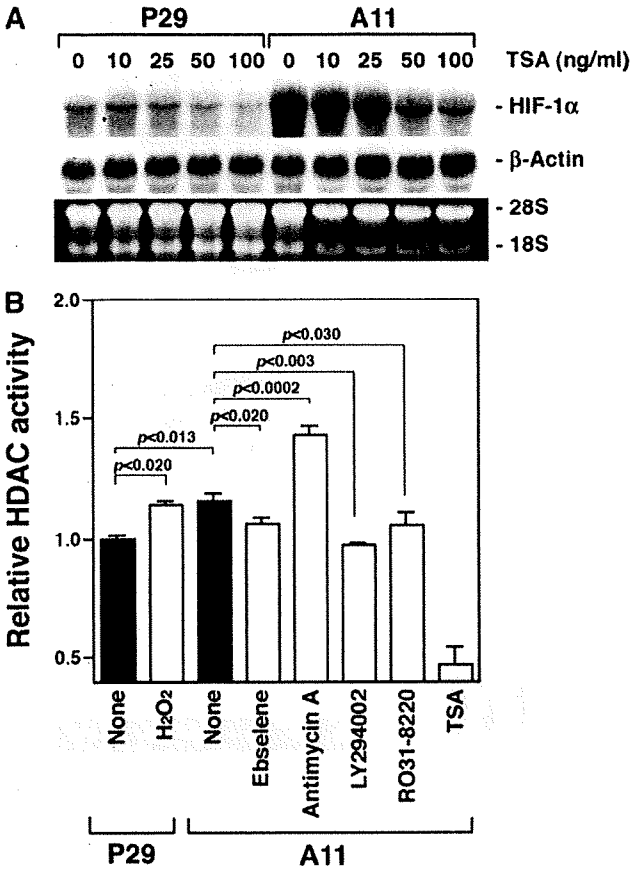

FIGURE 7. **HDAC activity is involved in the ROS-mediated *HIF-1α* transcription.** *A*, P29 and A11 cells were treated with TSA at the indicated concentrations for 18 h. Total RNA was extracted and subjected to Northern blot analysis. The blots were hybridized with a ^{32}P-labeled *HIF-1α* cDNA. Ethidium bromide staining of the gel is also shown. *B*, HDAC activity is shown in untreated P29 and P29 cells treated with 25 μM H_2O_2 for 16 h, and untreated A11 and A11 cells treated with ebselene (20 μM), antimycin A (20 μM), LY294002 (20 μM), Ro31-8220 (5 μM), and TSA (100 ng/ml) for 18 h.

HDAC pathway. Because mtDNA mutations have been implicated to be a factor in cancer etiology and shown to be gradually accumulated in tumor cells, some of them, especially pathogenic somatic mutations, may contribute to malignant progression by causing the up-regulation of HIF-1α protein in tumors.

REFERENCES

1. Brandon, M., Baldi, P., and Wallace, D. C. (2006) *Oncogene* **25,** 4647–4662
2. Park, J. S., Sharma, L. K., Li, H., Xiang, R., Holstein, D., Wu, J., Lechleiter, J., Naylor, S. L., Deng, J. J., Lu, J., and Bai, Y. (2009) *Hum. Mol. Genet.* **18,** 1578–1589
3. Dasgupta, S., Hoque, M. O., Upadhyay, S., and Sidransky, D. (2008) *Cancer Res.* **68,** 700–706
4. Ishikawa, K., Takenaga, K., Akimoto, M., Koshikawa, N., Yamaguchi, A., Imanishi, H., Nakada, K., Honma, Y., and Hayashi, J. (2008) *Science* **320,** 661–664
5. Semenza, G. L. (2009) *Semin. Cancer Biol.* **19,** 12–16
6. Semenza, G. L. (2008) *IUBMB Life* **60,** 591–597
7. Vaupel, P., and Mayer, A. (2007) *Cancer Metastasis Rev.* **26,** 225–239
8. Koshikawa, N., Iyozumi, A., Gassmann, M., and Takenaga, K. (2003) *Oncogene* **22,** 6717–6724
9. Secades, P., Rodrigo, J. P., Hermsen, M., Alvarez, C., Suarez, C., and Chiara, M. D. (2009) *Genes Chromosomes Cancer* **48,** 441–454
10. Saramäki, O. R., Savinainen, K. J., Nupponen, N. N., Bratt, O., and Visakorpi, T. (2001) *Cancer Genet. Cytogenet.* **128,** 31–34
11. Chandel, N. S., McClintock, D. S., Feliciano, C. E., Wood, T. M., Melendez, J. A., Rodriguez, A. M., and Schumacker, P. T. (2000) *J. Biol. Chem.* **275,** 25130–25138
12. Pagé, E. L., Robitaille, G. A., Pouysségur, J., and Richard, D. E. (2002) *J. Biol. Chem.* **277,** 48403–48409
13. Pouysségur, J., and Mechta-Grigoriou, F. (2006) *Biol. Chem.* **387,** 1337–1346
14. Klimova, T., and Chandel, N. S. (2008) *(2008) Cell Death Differ.* **15,** 660–666
15. Bonello, S., Zähringer, C., BelAiba, R. S., Djordjevic, T., Hess, J., Michiels, C., Kietzmann, T., and Görlach, A. (2007) *Arterioscler. Thromb. Vasc. Biol.* **27,** 755–761
16. Koshikawa, N., Maejima, C., Miyazaki, K., Nakagawara, A., and Takenaga, K. (2006) *Oncogene* **25,** 917–928
17. Luo, G., Gu, Y. Z., Jain, S., Chan, W. K., Carr, K. M., Hogenesch, J. B., and Bradfield, C. A. (1997) *Gene Expr.* **6,** 287–299
18. Indo, H. P., Davidson, M., Yen, H. C., Suenaga, S., Tomita, K., Nishii, T., Higuchi, M., Koga, Y., Ozawa, T., and Majima, H. J. (2007) *Mitochondrion* **7,** 106–118
19. Oh, Y. T., Lee, J. Y., Yoon, H., Lee, E. H., Baik, H. H., Kim, S. S., Ha, J., Yoon, K. S., Choe, W., and Kang, I. (2008) *Neurosci. Lett.* **431,** 155–160
20. Mayerhofer, M., Valent, P., Sperr, W. R., Griffin, J. D., and Sillaber, C. (2002) *Blood* **100,** 3767–3775
21. Frede, S., Stockmann, C., Freitag, P., and Fandrey, J. (2006) *Biochem. J.* **396,** 517–527
22. Kim, H. Y., Kim, Y. H., Nam, B. H., Kong, H. J., Kim, H. H., Kim, Y. J., An, W. G., and Cheong, J. (2007) *Exp. Cell Res.* **313,** 1866–1876
23. Iyer, N. V., Leung, S. W., and Semenza, G. L. (1998) *Genomics* **52,** 159–165
24. Minet, E., Ernest, I., Michel, G., Roland, I., Remacle, J., Raes, M., and Michiels, C. (1999) *Biochem. Biophys. Res. Commun.* **261,** 534–540
25. Das, C., and Kundu, T. K. (2005) *IUBMB Life* **57,** 137–149
26. Adcock, I. M. (2007) *Br. J. Pharmacol.* **150,** 829–831
27. Joseph, J., Mudduluru, G., Antony, S., Vashistha, S., Ajitkumar, P., and Somasundaram, K. (2004) *Oncogene* **23,** 6304–6315
28. Leoni, F., Zaliani, A., Bertolini, G., Porro, G., Pagani, P., Pozzi, P., Donà, G., Fossati, G., Sozzani, S., Azam, T., Bufler, P., Fantuzzi, G., Goncharov, I., Kim, S. H., Pomerantz, B. J., Reznikov, L. L., Siegmund, B., Dinarello, C. A., and Mascagni, P. (2002) *Proc. Natl. Acad. Sci. U.S.A.* **99,** 2995–3000
29. Yu, Z., Zhang, W., and Kone, B. C. (2002) *J. Am. Soc. Nephrol.* **13,** 2009–2017
30. Quivy, V., and Van Lint, C. (2004) *Biochem. Pharmacol.* **68,** 1221–1229
31. Noh, H., Oh, E. Y., Seo, J. Y., Yu, M. R., Kim, Y. O., Ha, H., and Lee, H. B. (2009) *Am. J. Physiol. Renal. Physiol.* **297,** 729–739
32. Witt, O., Deubzer, H. E., Milde, T., and Oehme, I. (2009) *Cancer Lett.* **277,** 8–21

THE JOURNAL OF BIOLOGICAL CHEMISTRY VOL. 284, NO. 51, pp. 35433–35440, December 18, 2009

TATA-binding Protein (TBP)-like Protein Is Engaged in Etoposide-induced Apoptosis through Transcriptional Activation of Human *TAp63* Gene*[S]

Received for publication, July 30, 2009, and in revised form, October 20, 2009 Published, JBC Papers in Press, October 26, 2009, DOI 10.1074/jbc.M109.050047

Yusuke Suenaga[‡§], Toshinori Ozaki[§], Yuji Tanaka[‡], Youquan Bu[§], Takehiko Kamijo[§], Takeshi Tokuhisa[¶], Akira Nakagawara[§1], and Taka-aki Tamura[‡2]

From the [‡]Graduate School of Science, Chiba University, 1-33 Yayoicho, Inage-ku, Chiba 263-8522, the [§]Division of Biochemistry, Chiba Cancer Center Research Institute, 666-2 Nitona, Chuoh-ku, Chiba 260-8717, and the [¶]Department of Developmental Genetics, Graduate School of Medicine, Chiba University, Chiba 260-8670, Japan

Accumulating evidence indicates that TBP (TATA-binding protein)-like protein (TLP) contributes to the regulation of stress-mediated cell cycle checkpoint and apoptotic pathways, although its physiological target genes have remained elusive. In the present study, we have demonstrated that human *TAp63* is one of the direct transcriptional target genes of TLP. Enforced expression of TLP results in the transcriptional induction of the endogenous *TAp63*, but not of the other *p53* family members such as *TAp73* and *p53*. Consistent with these results, small interference RNA-mediated knockdown led to a significant down-regulation of the endogenous *TAp63*. Luciferase reporter assay and chromatin immunoprecipitation analysis revealed that the genomic region located at positions −487 to −29, where +1 represents the transcriptional initiation site of *TAp63*, is required for TLP-dependent transcriptional activation of *TAp63* and also TLP is efficiently recruited onto this region. Additionally, cells treated with anti-cancer drug etoposide underwent apoptosis in association with the transcriptional enhancement of *TAp63* in a p53-independent manner, and the knockdown of the endogenous TLP reduced etoposide-induced apoptosis through repression of *TAp63* expression. Taken together, our present study identifies a TLP-TAp63 pathway that is further implicated in stress-induced apoptosis.

Transcriptional regulation involves the functional integration of diverse factors and is a critical regulatory step for cellular events that include growth, differentiation, and death. These cellular activities often occur simultaneously due to the action of regulatory factors with broad targets. A representative example of such a factor is the tumor suppressor p53 and its family members, including p63 and p73, which contribute to tumor suppression, cell cycle checkpoint, DNA repair, and apoptosis (1). p63 acts as a pro-apoptotic transcription factor (2, 3) and, like p53 and p73, is expressed as multiple isoforms (4). They include the *trans*-activating (TA)[3] isoform of p63, termed TAp63, and an NH_2-terminal activation domain-deficient isoform, ΔNp63, that acts as a dominant negative factor over p53, TAp63, and TAp73 (2). p63 has been clearly implicated in a variety of developmental processes (5), whereas its anticipated role as a tumor suppressor is unclear, mainly because of its low frequency of the somatic mutations in human tumors (6, 7). However, a study focused on long term effects of *p63* mutations in mice showed that mice bearing mutations in both *p63* and *p53* develop a more aggressive tumor, indicating the presence of a tumor suppressive activity of p63 (8). This is consistent with earlier studies indicating that p63 is required for p53-dependent apoptotic response (9) and that, in response to certain DNA damage insults, p63 activates an overlapping set of p53-target genes implicated in cell cycle arrest and apoptosis (10). Although extensive studies of p63 in human tumors have suggested that deregulated expression of TAp63 and ΔNp63 contributes to tumor development and progression (4), the precise molecular mechanisms behind the transcriptional regulation of *TAp63* remain to be unclear.

TATA-binding protein (TBP) is a general transcription factor that plays a central role in the regulation of pre-initiation complex formation by eukaryotic RNA polymerases (11, 12). Eukaryotic cells also contain multiple TBP paralogs implicated in transcriptional regulation during cell growth, differentiation, and development (11, 12). TBP-like protein (TLP) (13), also known as TBP-related factor 2 (14, 15), TLF (16), or TRP (17), is one of the TBP paralogs common to Metazoa and has been implicated by genetic studies in various developmental processes, including spermiogenesis in mice (11, 12). Although TLP fails to bind to TATA box (11, 12), it stimulates transcription from several TATA-less promoters (18). Mammalian TLP, unlike TBP, does not associate with TAFs to form a transcrip-

* This work was supported by a Grant-in-Aid from the Ministry of Health, Labor and Welfare for Third Term Comprehensive Control Research for Cancer (to A. N.), a Grant-in-Aid for Scientific Research on Priority Areas from the Ministry of Education, Culture, Sports, Science and Technology, Japan (to T. T. and A. N.), a Grant-in-Aid for Scientific Research from Japan Society for the Promotion of Science (to A. N.), and grants from Uehara Memorial Foundation and Futaba Corporation (to T. T. and A. N.).

[S] The on-line version of this article (available at http://www.jbc.org) contains supplemental Figs. S1–S3.

[1] To whom correspondence may be addressed: Division of Biochemistry, Chiba Cancer Center Research Institute, 666-2 Nitona, Chuou-ku, Chiba 260-8717, Japan. Tel.: 81-43-264-5431; Fax: 81-43-265-4459; E-mail: akiranak@chiba-cc.jp.

[2] To whom correspondence may be addressed. Tel.: 81-43-290-2823; Fax: 81-43-290-2824; E-mail: ttamura@faculty.chiba-u.jp.

[3] The abbreviations used are: TA, *trans*-activating isoform; ChIP, chromatin immunoprecipitation; FACS, fluorescence-activated cell sorter; NF1, neurofibromatosis type 1; siRNA, small interfering RNA; TBP, TATA-binding protein; TLP, TBP-like protein; TUNEL, terminal deoxynucleotidyl transferase-mediated dUTP nick end labeling; RT, reverse transcription.

tion factor IID-type complex but, instead, associates with TFIIA in cells (14, 19). It was reported earlier (20) that mammalian TLP activates transcription from the TATA-less neurofibromatosis type 1 (*NF1*) promoter through site-specific binding, but represses the TATA-containing c-*fos* promoter, thus leading to the prediction of an anti-oncogenic ability of TLP as well as the potential for direct binding to other target genes. Shimada *et al.* (21) reported that chicken TLP represses the G_2/M transition and, through its nuclear translocation, mediates apoptosis induction in a p53-independent manner. Hence, TLP is proposed to have both checkpoint and anti-oncogenic functions, although its physiological role and also the precise molecular mechanisms behind TLP-mediated apoptosis as well as cell cycle checkpoint remain to be elusive.

Here, we have analyzed mammalian TLP function in relation to TAp63 expression and show that TLP enhances the promoter activity of *TAp63* and thus leads to apoptosis. Further observations suggest that this novel TLP-TAp63 pathway increases the sensitivity to anti-cancer drug etoposide.

EXPERIMENTAL PROCEDURES

Cell Culture and Transfection—Chicken DT40 cells were grown in RPMI 1640 medium (Invitrogen) as previously described (21). DT40-TLP$^{-/-}$ cells derived from parental DT40 cells lack *TLP* (21). Human cervical carcinoma-derived HeLa and human hepatocellular carcinoma-derived HepG2 cells were cultured in Dulbecco's modified Eagle's medium (Invitrogen) supplemented with 10% heat-inactivated fetal bovine serum (Invitrogen), penicillin (100 IU/ml), and streptomycin (100 μg/ml). Human hepatocellular carcinoma-derived Hep3B cells were grown in RPMI 1640 medium supplemented with 10% heat-inactivated fetal bovine serum and antibiotics. HepG2 and HeLa cells carry wild-type *p53*. Hep3B and DT40 cells lack *p53*. Where indicated, cells were exposed to etoposide (at a final concentration of 50 μM). For transfection, DT40 cells were transiently transfected with the indicated expression plasmids by electroporation. HeLa cells were transiently transfected with the indicated combinations of the expression plasmids using Lipofectamine 2000 transfection reagent (Invitrogen) according to the manufacturer's instructions.

RT-PCR—Total RNA was prepared from the indicated cells using RNeasy Mini Kit (Qiagen, Valencia, CA) according to the manufacturer's recommendations. For the RT-PCR, first strand cDNA was generated using SuperScript II reverse transcriptase (Invitrogen) and random primers. The resultant cDNA was subjected to the PCR-based amplification. The oligonucleotide primers used in this study were as follows: human *TLP*, 5′-CCTCTTCCCACGGATGTGAT-3′ (sense) and 5′-GAGTCCAATGTGCAGCAGT-3′ (reverse); mouse *TLP*, 5′-GCCATTTGAACTTAAGGA-3′ (forward) and 5′-TGTAAATTCTGGCAA-3′ (reverse); human *TAp63*, 5′-GTCCCAGAGCACACAGACAA-3′ (forward) and 5′-GAGGAGCCGTTCTGAATCTG-3′ (reverse); chicken *TAp63*, 5′-GAAACAGCCATGCCCAGTAT-3′ (forward) and 5′-CAAATGCGAGCTTCAAAACA-3′ (reverse); human *TAp73*, 5′-CGGGACGGACGCCGATG-3′ (forward) and 5′-GAAGGTCGAAGTAGGTGCTGTCTGG-3′ (reverse); human *p53*, 5′-ATTTGATGCTGTCCCCGGACGATATTGAAC-3′ (forward) and 5′-ACCCTTTTTGGACTTCCGGACGATATTGAAC-3′ (reverse); human p21^{waf1}, 5′-GACACCACTGGAGGGTGACT-3′ (forward) and 5′-CCCTAGGCTGTGCTCACTTC-3′ (reverse); human 14-3-3σ, 5′-AGAGCGAAACCTGCTCTCAG-3′ (forward) and 5′-CTCCTTGATGAGGTGGCTGT-3′ (reverse); human *Lamin A/C*, 5′-CCGAGTCTGAAGAGGTGGTC-3′ (forward) and 5′-AGGTCACCCTCCTTCTTGGT-3′ (reverse); human *BAX*, 5′-TCTGACGCAACTTCAACAC-3′ (forward) and 5′-GAGGAGTCTCACCCAACCAC-3′ (reverse); human *PUMA*, 5′-GCCCAGACTGTGAATCCTGT-3′ (forward) and 5′-TCCTCCCTCTTCCGAGATTT-3′ (reverse); human *NOXA*, 5′-GCAAGAATGGAAGACCCTTG-3′ (forward) and 5′-GTGCTGAGTTGGCACTGAAA-3′ (reverse); human *GAPDH*, 5′-ACCTGACCTGCCGTCTAGAA-3′ (forward) and 5′-TCCACCACCCTGTTGCTGTA-3′ (reverse). The expression of β-*actin* or *GAPDH* was measured as an internal control. The PCR products were subjected to 1% agarose gel electrophoresis and visualized by ethidium bromide staining.

Real-time Quantitative RT-PCR—Total RNA was extracted from clinical samples using TRIzol reagent (Invitrogen) according to the manufacturer's instructions, and reverse transcription was performed with SuperScript II reverse transcriptase (Invitrogen). Real-time quantitative PCR (TaqMan PCR) using an ABI Prism 7700 sequence detection system (Perkin-Elmer Applied Biosystems, Foster City, CA) was carried out according to the manufacturer's protocol. All the reactions were performed in triplicate. The data were averaged from the values obtained in each reaction. The mRNA levels of each of the genes were standardized by β-*actin*.

siRNA—Hep3B cells transiently transfected with siRNA targeting TLP (TLP siRNA-1, 5′-UAACAGGGCCCAAUGUAAA-3′; TLP siRNA-2, 5′-GGAAGGAGCAAAUGUAAUU-3′), siRNA against TAp63 (TAp63 siRNA-1, 5′-CAGCUAUAUGUUCAGUUC-3′; TAp63 siRNA-2, 5′-GAUUGAGAUUAGCAUGGAC-3′) (Invitrogen) or with siRNA against Lamin A/C (Dharmacon, Chicago, IL) by using Lipofectamine RNAiMAX transfection reagent (Invitrogen) according to the manufacturer's instructions. Forty-eight hours after transfection, total RNA was prepared and processed for RT-PCR.

Immunoblotting—Cells were washed in ice-cold phosphate-buffered saline and lysed in an SDS-sample buffer. After brief sonication, whole cell lysates were boiled for 5 min, resolved by 12% SDS-PAGE, and electrotransferred onto Immobilon-P membranes (Millipore, Bedford, MA). The membranes were blocked with Tris-buffered saline containing 0.1% Tween 20 and 5% nonfat dry milk and then incubated with monoclonal anti-p21^{waf1} (Ab-1, Oncogene Research Products, Cambridge, MA), monoclonal anti-FLAG (M2, Sigma), monoclonal anti-Lamin B (Ab-1, Calbiochem), monoclonal anti-tubulin-α (Ab-2, Neomarkers, Fremont, CA), polyclonal anti-TAp63 (22), polyclonal anti-TLP (23), or with polyclonal anti-actin (20-33, Sigma) antibody for 1 h at room temperature followed by an incubation with the appropriate horseradish peroxidase-conjugated secondary antibodies (Jackson ImmunoResearch Laboratories, West Grove, PA) for 1 h at room temperature. The

chemiluminescence reaction was performed using ECL reagent (Amersham Biosciences, Piscataway, NJ).

Construction of Luciferase Reporter Plasmids—A luciferase reporter plasmid containing *TAp63* promoter region encompassing from −2340 to +26, where +1 represents the transcriptional initiation site, was amplified by PCR-based strategy using genomic DNA prepared from human placenta as a template. Oligonucleotide primers used were as follows: F1, 5′-TTGGTAGAGCTCGAGGATAGCTTGAGTCCAGCAG-3′ (forward) and R1, 5′-AGATATCCCTTTCACATCCC-3′ (reverse); F2, 5′-GTGCATGTGTTTGAGGTAGG-3′ (forward) and R2, 5′-CTTAGAGCTAGCCCTTCAACTGTCTTTGATATCAACG-3′ (reverse). Underlined sequences indicate the positions of SacI restriction site in the forward primer F1 and NheI restriction site in the reverse primer R2. PCR products were gel-purified and subcloned into pGEM-T Easy plasmid (Promega, Southampton, UK) according to the manufacturer's protocol. The resultant plasmid DNA was digested with SacI plus HindIII or with HindIII plus NheI and then subcloned into SacI/NheI restriction sites of pGL3-basic plasmid (Promega) to give pGL3-TAp63(−2340). A series of the 5′ deletion mutants of pGL3-TAp63(−2340) were generated by using an Erase-A-Base system (Promega) according to the manufacturer's instructions.

Luciferase Reporter Assay—HeLa cells were transiently co-transfected with the constant amount of the indicated pGL3-TAp63 luciferase reporter constructs (100 ng), pRL-TK *Renilla* luciferase reporter plasmid (10 ng) together with or without 100 ng of the expression plasmid for FLAG-TLP. The total amount of the plasmid DNA per each transfection was kept constant (510 ng) with the empty plasmid (pCIneo). Forty-eight hours after transfection, cells were harvested and lysed, and both firefly and *Renilla* luciferase activities were measured by using a Dual-Luciferase reporter assay system (Promega). The firefly luminescence signal was normalized based on the *Renilla* luminescence signal.

ChIP Assay—Chromatin immunoprecipitation (ChIP) assay was performed according to the protocol provided by Upstate Biotechnology (Charlottesville, VA). In brief, HeLa cells were transiently transfected with the expression plasmid for FLAG-TLP. Forty-eight hours after transfection, cells were cross-linked with 1% formaldehyde in medium at 37 °C for 15 min. Cells were then washed in ice-cold phosphate-buffered saline and resuspended in 200 μl of SDS lysis buffer containing protease inhibitor mixture. The suspension was sonicated on ice and pre-cleared with protein A-agarose beads blocked with sonicated salmon sperm DNA (Upstate Biotechnology) for 30 min at 4 °C. The beads were removed, and the chromatin solution was immunoprecipitated with polyclonal anti-FLAG (Sigma) antibody at 4 °C, followed by incubation with protein A-agarose beads for an additional 1 h at 4 °C. The immune complexes were eluted with 100 μl of elution buffer (1% SDS and 0.1 M $NaHCO_3$), and formaldehyde cross-links were reversed by heating at 65 °C for 6 h. Proteinase K was added to the reaction mixtures and incubated at 45 °C for 1 h. DNA of the immunoprecipitates and control input DNA were purified and then analyzed by standard PCR using human *TAp63* promoter-specific primers.

Subcellular Fractionation—To prepare nuclear and cytoplasmic extracts, cells were lysed in 10 mM Tris-HCl, pH 7.5, 1 mM EDTA, 0.5% Nonidet P-40, 1 mM phenylmethylsulfonyl fluoride, and a protease inhibitor mix (Sigma) and centrifuged at 5000 rpm for 10 min to collect soluble fractions, which were referred to as cytosolic extracts. Insoluble materials were washed in the lysis buffer and further dissolved in SDS-sample buffer to collect the nuclear extracts. The nuclear and cytoplasmic fractions were subjected to the immunoblot analysis using monoclonal anti-Lamin B (Ab-1, Oncogene Research Products) or monoclonal anti-tubulin-α (Ab-2, Neomarkers) antibody.

TUNEL Staining—Hep3B cells were grown on coverslips and transiently transfected with the indicated siRNAs. Forty-eight hours after transfection, cells were fixed in 4% paraformaldehyde and apoptotic cells were detected by using an *in situ* cell detection Kit (Roche Molecular Biochemicals, Mannheim, Germany) according to the manufacturer's protocol. The coverslips were mounted with 4′,6-diamidino-2-phenylindole-containing mounting medium (Vector Laboratories, Burlingame, CA) and observed under a Fluoview laser scanning confocal microscope (Olympus, Tokyo, Japan).

FACS Analysis—Transfected HepG2 cells were exposed to 50 μM of etoposide. Forty-eight hours after the treatment, floating and attached cells were collected, washed in ice-cold phosphate-buffered saline, and fixed in 70% ethanol at −20 °C. Following incubation with phosphate-buffered saline containing 40 μg/ml of propidium iodide and 200 μg/ml of RNase A for 1 h at room temperature in the dark, stained nuclei were analyzed by a FACScan machine (BD Biosciences, Mountain View, CA).

Statistical Analysis—The data obtained from real-time PCR were expressed as means ± S.E. of the mean.

RESULTS

TLP Has an Ability to Induce the Expression of TAp63—We have previously described that TLP induces both cell cycle arrest and apoptosis in chicken DT40 cells in a p53-independent manner (21). These results imply that the other p53 family members such as p73 or p63 could be closely involved in these cellular processes, because p53 family members play a dominant role in the regulation of cell fate determination. To examine the possible contribution of TLP to *p53*, *TAp73*, and *TAp63* gene expression, human cervical carcinoma-derived HeLa cells were transiently transfected with FLAG-TLP expression plasmid. Intriguingly, enforced expression of FLAG-TLP resulted in a significant up-regulation of *TAp63* but not of *p53* and *TAp73* (Fig. 1, *A* and *B*). Consistent with these results, siRNA-mediated knockdown of the endogenous *TLP* led to a remarkable down-regulation of the endogenous *TAp63* as well as its direct transcriptional target genes such as $p21^{waf1}$ and *NOXA* (Fig. 1*C*). $p21^{waf1}$ and NOXA are involved in the induction of cell cycle arrest and apoptosis, respectively (24). Additionally, knocking down of the endogenous *TAp63* had an undetectable effect on the expression level of the endogenous *TLP*, whereas the expression levels of the endogenous $p21^{waf1}$ and *NOXA* dramatically decreased. In support with these results, *TLP*-deficient chicken DT40 cells expressed *p63* at an extremely lower level as compared with wild-type DT40 cells, and ectopic

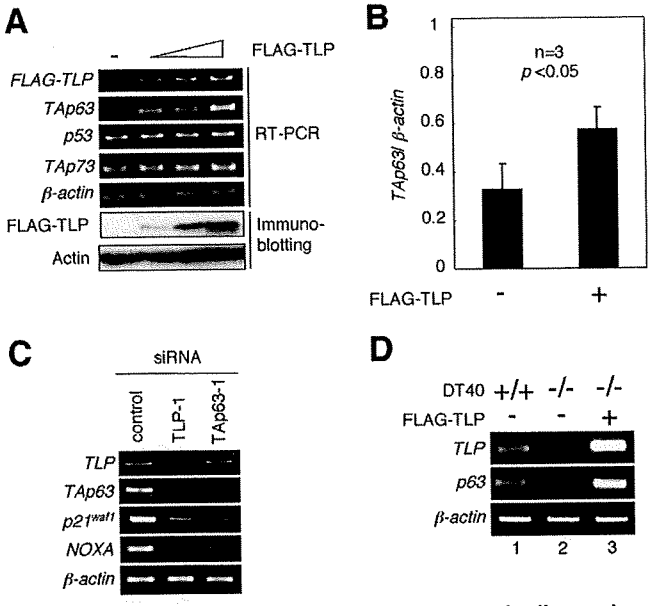

FIGURE 1. **Effects of ectopic expression of TLP on *p53* family members.** *A*, enforced expression of FLAG-TLP results in the up-regulation of *TAp63* but not of *p53* and *TAp73*. Human cervical carcinoma-derived HeLa cells were transiently transfected with or without the increasing amounts of FLAG-TLP expression plasmid (1.0, 1.5, or 2.0 μg). As a negative control, the empty plasmid (2.0 μg) was introduced into HeLa cells (−). Forty-eight hours after transfection, total RNA and whole cell lysates were prepared and analyzed by semi-quantitative RT-PCR using the indicated primers and immunoblotting with anti-FLAG antibody, respectively. For RT-PCR, *β-actin* was used as an internal control. For immunoblotting, actin was used as a loading control. *B*, quantitative real-time RT-PCR analysis. HeLa cells were transiently transfected with the constant amount of the empty plasmid or with the expression plasmid encoding FLAG-TLP (2.0 μg). Forty-eight hours after transfection, the expression levels of *TAp63* were examined by quantitative real-time RT-PCR using *β-actin* as an internal control. Data represent -fold induction of *TAp63* mRNA levels relative to those of *β-actin* mRNA. *C*, siRNA-mediated knockdown of the endogenous TLP. Human hepatocellular carcinoma-derived Hep3B cells were transiently transfected with 10 nM of control siRNA, siRNA against *TLP* (TLP-1) or with siRNA targeting *TAp63* (TAp63–1). Forty-eight hours after transfection, total RNA was prepared and subjected to semi-quantitative RT-PCR. *β-actin* was used as an internal control. *D*, a significant correlation between the expression levels of *TLP* and *TAp63*. Chicken wild-type DT40 cells and TLP-deficient DT40 cells were transiently transfected with the empty plasmid (−) or with the expression plasmid for FLAG-TLP (+). Forty-eight hours after transfection, total RNA was prepared and processed for semi-quantitative RT-PCR. *β-actin* was used as an internal control.

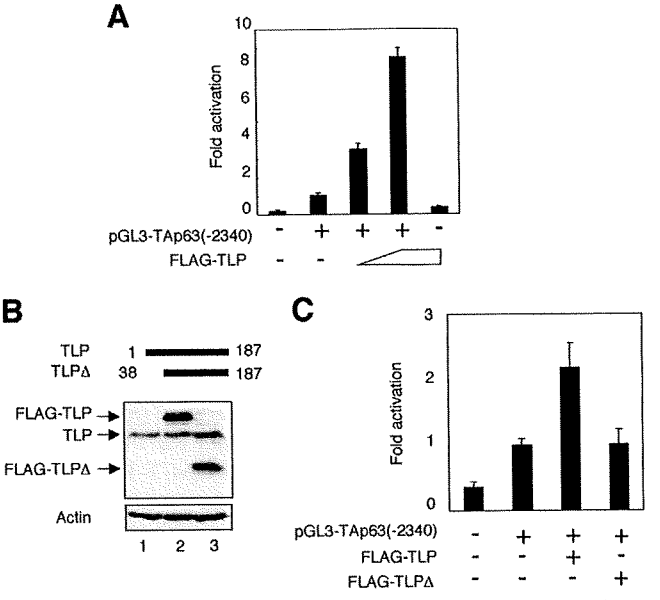

FIGURE 2. **NH_2-terminal deletion mutant of TLP fails to transactivate *TAp63* promoter.** *A*, pGL3-TAp63(−2340) responds to TLP. HeLa cells were transiently co-transfected with the constant amount of the luciferase reporter plasmid termed pGL3-TAp63(−2340) (100 ng) and *Renilla* luciferase reporter plasmid (pRL-TK, 10 ng) along with or without the increasing amounts of the expression plasmid encoding FLAG-TLP (100 or 200 ng). Forty-eight hours after transfection, cells were lysed and their luciferase activities were examined. Firefly luminescence signal was normalized based on the *Renilla* luminescence signal. Results are shown as -fold induction of the firefly luciferase activity compared with control cells transfected with the empty plasmid. *B*, immunoblotting. HeLa cells were transiently transfected with the constant amount of the empty plasmid (*lane 1*), the expression plasmid for FLAG-TLP (*lane 2*), or with the expression plasmid encoding FLAG-TLPΔ (*lane 3*). Forty-eight hours after transfection, whole cell lysates were analyzed by immunoblotting with the anti-TLP antibody. Actin was used as a loading control. *C*, luciferase reporter assay. HeLa cells were transiently co-transfected with the constant amount of pGL3-TAp63(−2340) and *Renilla* luciferase reporter plasmid along with or without the expression plasmid for FLAG-TLP or FLAG-TLPΔ. Forty-eight hours after transfection, cells were lysed and their luciferase activities were determined as in *A*.

expression of FLAG-TLP in *TLP*-deficient DT40 cells caused an increase in the expression level of *p63* (Fig. 1*D*). Thus, it is likely that *TAp63* is one of direct transcriptional target genes of TLP.

Identification of the Region within Human TAp63 Promoter Required for TLP-mediated Transactivation of TAp63—To identify the essential region within human *TAp63* promoter required for TLP-dependent transcriptional activation of *TAp63*, we have generated the luciferase reporter plasmid bearing *TAp63* genomic fragment spanning from positions −2340 to +26, where +1 represents the transcriptional initiation site, termed pGL3-TAp63(−2340). HeLa cells were transiently co-transfected with the constant amount of pGL3-TAp63(−2340), *Renilla* luciferase reporter plasmid together with or without the increasing amounts of the expression plasmid for FLAG-TLP. Forty-eight hours after transfection, cells were lysed, and their luciferase activities were measured. As shown in Fig. 2*A*, FLAG-TLP had an ability to enhance the luciferase activity driven by *TAp63* promoter in a dose-dependent manner. Similar results were also obtained in *p53*-deficient human lung carcinoma-derived H1299 cells (data not shown). In addition, NH_2-terminal deletion mutant of TLP (FLAG-TLPΔ) (Fig. 2*B*), which lacks a transcriptional activation function, failed to transactivate *TAp63* promoter as examined by luciferase reporter assay (Fig. 2*C*). These observations suggest that the genomic region of *TAp63* gene used in the luciferase reporter assay contains one or more TLP-responsive elements.

To further extend our study, a series of progressively 5′-truncated *TAp63* promoter reporter constructs were generated and subjected to luciferase reporter assay. As clearly shown in Fig. 3*A*, deletion up to −731 and −28 resulted in a significant decrease in the luciferase activity driven by *TAp63* promoter, indicating that there exist at least two independent genomic regions of *TAp63* gene (−1101 to −732 and −487 to −29) required for TLP-dependent transactivation of *TAp63*. To examine whether TLP could be recruited onto the essential genomic region of *TAp63* promoter, which we have identified, we performed a ChIP assay. For this purpose, we have designed four primer sets (#1, #2, #3, and #4) to amplify the indicated genomic regions of *TAp63* promoter (Fig. 3*B*). HeLa cells were

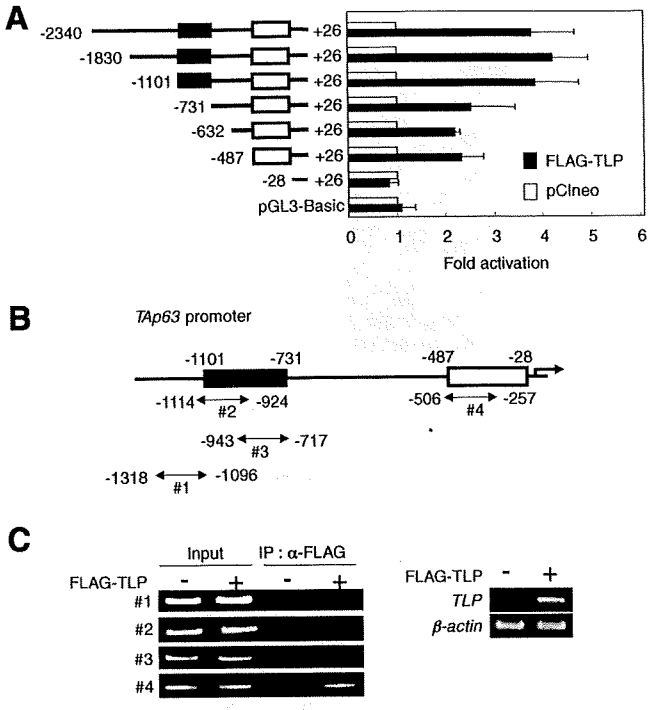

FIGURE 3. **Identification of region(s) within human *TAp63* promoter required for TLP-dependent transcriptional activation.** *A*, luciferase reporter assays. HeLa cells were transiently co-transfected with the constant amount of the indicated luciferase reporter constructs bearing various length of human *TAp63* promoter region (100 ng) and *Renilla* luciferase reporter plasmid (pRL-TK, 10 ng) together with the empty plasmid (pCIneo) or with the expression plasmid for FLAG-TLP. Forty-eight hours after transfection, cells were lysed and their luciferase activities were measured as described in the legend for Fig. 2. *Filled* and *open boxes* indicate the putative TLP-responsive regions within *TAp63* promoter. *B*, schematic drawing of *TAp63* promoter region. *Filled* and *open boxes* indicate the putative TLP-responsive regions within *TAp63* promoter. The positions of primer sets (*#1*, *#2*, *#3*, and *#4*) relative to the transcriptional initiation site (+1) used for ChIP assay are indicated. *C*, ChIP assay. HeLa cells were transiently transfected with the empty plasmid or with the expression plasmid for FLAG-TLP. Expression of *FLAG-TLP* was confirmed by semi-quantitative RT-PCR (*right panels*). Forty-eight hours after transfection, cells were cross-linked with formaldehyde and cross-linked chromatin was sonicated followed by immunoprecipitation with anti-FLAG antibody. Genomic DNA was purified from the immunoprecipitates and subjected to PCR using the indicated primer sets.

transiently transfected with the empty plasmid or with the expression plasmid for FLAG-TLP. Forty-eight hours after transfection, chromatin DNA was cross-linked and then processed for ChIP assay. The expression of the exogenous FLAG-TLP was examined by semi-quantitative RT-PCR (Fig. 3*C*, *right panel*). As clearly shown in Fig. 3*C*, genomic DNA extending from −506 to −257 was specifically amplified, suggesting that TLP is efficiently recruited onto the proximal promoter region of the human *TAp63* gene (−487 to −29) and that the upstream sequences (−1101 to −732) might act to enhance the function of the TLP-bound downstream sequences.

Identification of the Putative TLP-responsive Element within the Proximal Region of TAp63 Promoter—During the extensive search of the proximal region of human *TAp63* promoter, we have found out the sequence element (5′-AGCTGGAGCA-3′), which was also included within one of the TLP-binding sequences of *NF1* gene (5′-AGCTGAGAGCA-3′). Of note, this sequence element was well conserved among mouse, chicken, and dog *TAp63* promoter regions (over 80% sequence identity). To address the functional significance of this sequence element in the regulation of TLP-dependent transcriptional enhancement of *TAp63* gene, we have generated a luciferase reporter plasmid bearing mutant *TAp63* promoter in which the putative TLP-responsive element (5′-AGCTGGAGCA-3′) was substituted to the mutant sequence (5′-CTAGTGAGCA-3′) (pGL3-TAp63(−2340/M1)). HeLa cells were transiently transfected with the constant amount of pGL3-TAp63(−2340) or pGL3-TAp63(−2340/M1) along with the expression plasmid for FLAG-TLP or with the empty plasmid. As shown in Fig. 4*A*, introduction of mutations into the putative TLP-responsive element decreased the luciferase activity mediated by exogenously expressed FLAG-TLP, suggesting that this sequence element might act as a TLP-responsive element for the human *TAp63* gene.

To further confirm this issue, we have inserted four tandem repeats of the putative TLP-responsive element or mutant form of the putative TLP-responsive element into just upstream of *TAp63* core promoter region to give pGL3-TAp63-TLP-luc and pGL3-TAp63-M1-luc, respectively. As shown in Fig. 4*B*, luciferase reporter assays demonstrated that pGL3-TAp63-TLP-luc but not pGL3-TAp63-M1-luc responds to the exogenously expressed FLAG-TLP, suggesting that the putative TLP-responsive element found in the present study plays an essential role in the regulation of TLP-dependent transactivation of *TAp63*.

Etoposide-mediated Induction of TLP and TAp63 in p53-deficient Cells—It has been shown that TAp63 is induced in human hepatocellular carcinoma-derived *p53*-deficient Hep3B cells in response to etoposide and also involved in the promotion of apoptosis (25, 26). We therefore investigated the effects of etoposide on the expression level of TAp63 and TLP in Hep3B cells. To this end, Hep3B cells were exposed to etoposide at a final concentration of 50 μM. At the indicated time points after etoposide treatment, total RNA and whole cell lysates were prepared and subjected to semi-quantitative RT-PCR and immunoblotting, respectively. As shown in Fig. 5*A*, the expression level of the endogenous *TLP* was induced in response to etoposide in association with the up-regulation of *TAp63* as well as its transcriptional target genes such as $p21^{waf1}$, *14-3-3σ*, *NOXA*, *PUMA*, and *BAX*. Similarly, etoposide treatment led to a remarkable induction of the endogenous TLP protein as well as TAp63 protein and its target gene products, including $p21^{waf1}$ and NOXA (Fig. 5*B*). Similar results were also obtained in human hepatocellular carcinoma-derived HepG2 cells (supplemental Fig. S1).

Consistent with our previous observations (27), TLP accumulated in cell nucleus of Hep3B cells in response to etoposide as examined by immunoblotting (Fig. 5*C*). Similar results were also obtained in HepG2 cells (supplemental Fig. S1). Next, we sought to examine whether the endogenous TLP could be recruited onto *TAp63* promoter in response to etoposide. For this purpose, Hep3B cells were treated with or without 50 μM etoposide. Forty-eight hours after etoposide treatment, cells were cross-linked and the immunoprecipitated genomic DNA was subjected to ChIP assay. As shown in Fig. 5*D*, the endogenous TLP was induced to be recruited onto *TAp63* promoter region in response to etoposide. Because it has been shown that

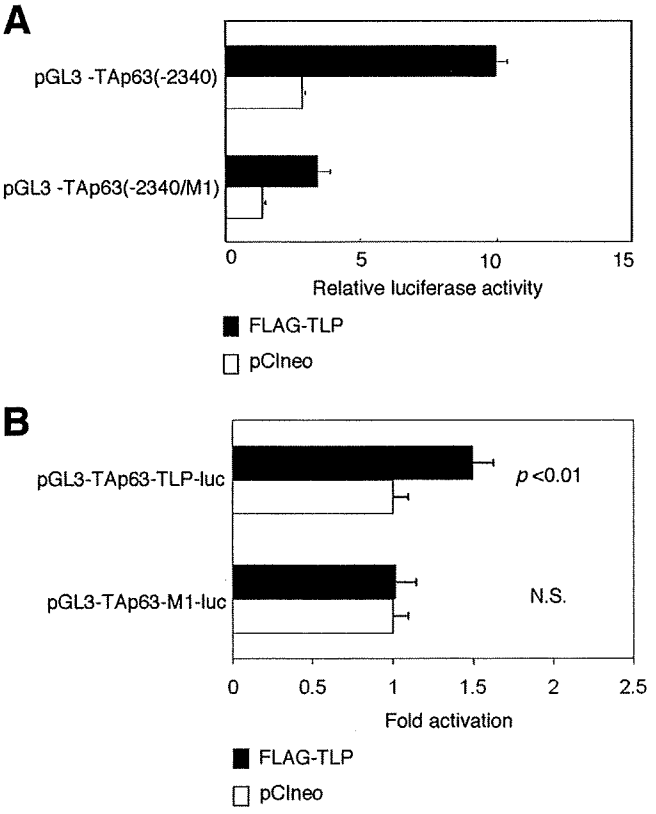

FIGURE 4. **TLP-responsive element within human *TAp63* promoter.** *A*, introduction of the mutations into the putative TLP-responsive element. We have introduced the mutations (5′-CTAGTGAGCA-3′) into the putative TLP-responsive element (5′-AGCTGGAGCA-3′) within pGL3-TAp63(−2340) to give pGL3-TAp63(−2340/M1). HeLa cells were transiently co-transfected with the constant amount of *Renilla* luciferase reporter plasmid together with pGL3-TAp63(−2340) or with pGL3-TAp63(−2340) in the presence of the expression plasmid for FLAG-TLP (*closed bars*) or empty plasmid (*open bars*). Forty-eight hours after transfection, cells were lysed and their luciferase activities were measured. *B*, functional significance of the putative TLP-responsive element. We have generated the luciferase reporter construct bearing four tandem repeats of the putative TLP-responsive element (5′-AGCTGGAGCA-3′) fused to just upstream of *TAp63* core promoter termed pGL3-TAp63-TLP-luc and its mutant carrying four tandem repeats of mutant form of the canonical TLP-responsive element (5′-CTAGTGAGCA-3′) fused to just upstream of *TAp63* core promoter termed pGL3-TAp63-M1-luc. HeLa cells were transiently co-transfected with the constant amount of *Renilla* luciferase reporter plasmid along with the constant amount of pGL3-TAp63-TLP-luc or with pGL3-TAp63-M1-luc in the presence of FLAG-TLP expression plasmid or the empty plasmid. Eighteen hours after transfection, cells were lysed, and their luciferase activities were determined. *Open* and *closed bars* indicate the relative luciferase activity in cells transfected with the empty plasmid and the expression plasmid for FLAG-TLP, respectively. *N.S.*, not significant.

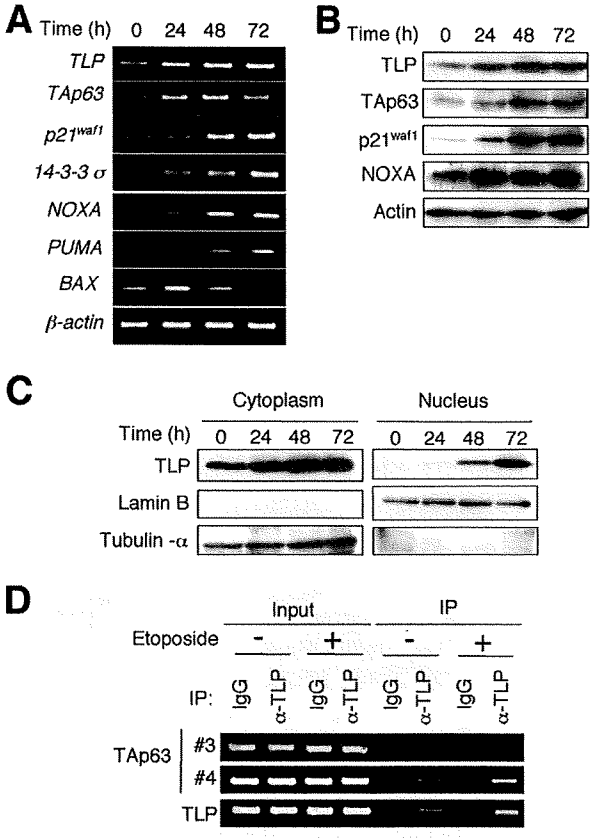

FIGURE 5. **TLP and TAp63 are induced in response to DNA damage.** *A*, etoposide treatment results in a significant induction of *TLP* and *TAp63*. Hep3B cells were treated with 50 μM of etoposide or left untreated. At the indicated time points after etoposide treatment, total RNA was prepared and subjected to semi-quantitative RT-PCR. *B*, immunoblotting. Hep3B cells were exposed to 50 μM of etoposide. At the indicated time points after exposure to etoposide, whole cell lysates were prepared and processed for immunoblotting with the indicated antibodies. *C*, etoposide-mediated nuclear accumulation of TLP. Hep3B cells were exposed to 50 μM etoposide. At the indicated time points after etoposide treatment, cells were biochemically fractionated into nuclear and cytoplasmic fractions followed by immunoblotting with anti-TLP antibody. Lamin B and tubulin-α were used as nuclear and cytoplasmic markers, respectively. *D*, ChIP assay. Hep3B cells were treated with 50 μM etoposide or left untreated. Forty-eight hours after etoposide treatment, cells were cross-linked with formaldehyde and cross-linked chromatin was sonicated followed by immunoprecipitation with normal goat IgG or with polyclonal anti-TLP antibody. Genomic DNA was purified from the immunoprecipitates and subjected to PCR using the indicated primer sets as described in the legend for Fig. 3.

TLP has an ability to transactivate its own promoter (28), we examined the recruitment of TLP onto its promoter region as a positive control (*bottom panel* of Fig. 5*D*).

The Effect of Knocking Down of the Endogenous TLP or TAp63 on Etoposide-mediated Apoptosis—To examine the functional significance of the endogenous TLP and TAp63 in the regulation of etoposide-mediated apoptosis, Hep3B cells were transiently transfected with control siRNA, siRNA against TLP (TLP-1), or with siRNA targeting TAp63 (TAp63–1). Forty-eight hours after transfection, cells were exposed to etoposide for 48 h. As seen in Fig. 6*A*, knocking down of the endogenous TLP resulted in a significant down-regulation of the endogenous TAp63 as well as its target gene products such as $p21^{waf1}$ and NOXA. Similarly, siRNA-mediated knockdown of the endogenous TAp63 caused a remarkable reduction in the expression level of $p21^{waf1}$ and NOXA, suggesting that the TLP/TAp63 pathway contributes to the promotion of apoptosis mediated by etoposide. Consistent with this notion, TUNEL staining experiments demonstrated that knocking down of the endogenous TLP or TAp63 results in a significant reduction of number of TUNEL-positive cells as compared with that of control cells (Fig. 5*B*). Similar results were obtained in Hep3B cells transfected with the different set of siRNA (supplemental Fig. S2) and also obtained in HepG2 cells (supplemental Fig. S3). Taken together, our present findings strongly suggest that TLP has an ability to induce etoposide-mediated apoptosis through up-regulation of TAp63 expression.

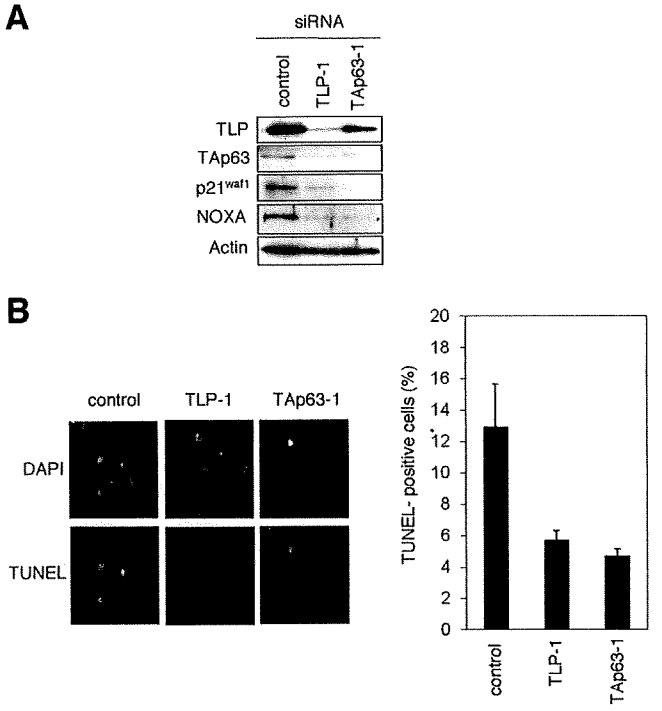

FIGURE 6. **Effects of the endogenous TLP and TAp63 in the regulation of DNA damage response.** *A*, siRNA-mediated knockdown of the endogenous TLP and TAp63. Hep3B cells were transiently transfected with 10 nM control siRNA, siRNA against *TLP* (TLP-1) or with siRNA targeting *TAp63* (TAp63-1). Forty-eight hours after transfection, cells were exposed to 50 μM etoposide. Forty-eight hours after etoposide treatment, whole cell lysates were prepared and processed for immunoblotting with indicated antibodies. *B*, TUNEL staining. Hep3B cells were transiently transfected as in *A*. Forty-eight hours after transfection, cells were exposed to 50 μM etoposide. Forty-eight hours after etoposide treatment, cells were fixed in 4% parafolmaldeyde and subjected to TUNEL staining. Cell nuclei were stained with 4′,6-diamidino-2-phenylindole (*DAPI*). The percentage of TUNEL-positive cells shown in each *column* represents the mean of three independent experiments (*right panels*).

DISCUSSION

Considering that TBP has an essential role in the regulation of basal transcription, TBP-related factors, including TLP might also participate in the transcriptional regulatory mechanisms. Previously, it has been shown that TBP is directly associated with tumor suppressor p53, and their complex formation contributes to the successful transcription (29). Although we have described that TLP has an intrinsic ability to prolong the G_2 phase and to induce apoptosis in a p53-independent manner (21), our earlier study did not rule out the possible involvement of the other p53 family members such as TAp73 and TAp63 in this process. In the present study, we have found for the first time that, upon DNA damage mediated by anti-cancer drug etoposide, TLP is induced to accumulate in cell nucleus in association with a significant up-regulation of *TAp63* as well as its direct target genes, suggesting that TLP acts as a transcriptional activator for pro-apoptotic TAp63.

According to our present results, ectopic expression of FLAG-TLP led to a significant induction of *TAp63* but not of the other *p53* family members such as *p53* and *TAp73*, indicating that TLP acts as a specific transcriptional activator for TAp63. Consistent with these observations, siRNA-mediated knockdown of the endogenous TLP resulted in a remarkable down-regulation of *TAp63*. In addition, TLP had an undetectable effect on SV40 promoter (data not shown). Intriguingly, TLP-dependent transcriptional up-regulation was also observed in chicken DT40 cells, suggesting that the molecular mechanisms behind TLP-dependent transcriptional up-regulation of *TAp63* are conserved among various species. By using luciferase reporter assays, we have identified the proximal and distal regions within human *TAp63* promoter required for TLP-dependent transcriptional activation of *TAp63*. Among them, TLP was efficiently recruited onto the proximal region but not onto the distal region as examined by ChIP assay. Thus, we have focused our attention on the proximal region for further analysis. Chong *et al.* described that TLP has an ability to transactivate *NF1* gene promoter, and they have identified the small independent two regions within *NF1* promoter required for TLP-dependent transcriptional activation of *NF1* gene (20). Based on their results, the above-mentioned two sequences directly bound to the purified TLP prepared from HeLa cells. During the extensive search of the proximal region of *TAp63* promoter, we have found out the sequence element (5′-AGCTGGAGCA-3′), which was also included within one of the TLP-binding sequences of *NF1* gene (5′-AGCTGAGAGCA-3′). Of note, this sequence element was well conserved among mouse, chicken, and dog *TAp63* promoter regions (over 80% sequence identity). Introduction of mutations into this sequence element decreased the luciferase activity mediated by exogenously expressed FLAG-TLP, suggesting that this sequence element might act as a TLP-responsive element for human *TAp63* gene.

As mentioned above, the distal region of *TAp63* promoter had an indirect effect on TLP-dependent transcriptional regulation of *TAp63*. Consistent with these results, pGL3-TAp63(−2340/M1) in which mutations were introduced into the proximal TLP-responsive element retained an ability to respond to the exogenously expressed FLAG-TLP but to the lesser degree. This might be due to the presence of the additional regulatory sequence(s) within *TAp63* promoter, including the distal region. When the four putative TLP-responsive elements were fused to core SV40 promoter, luciferase activity was undetectable in response to exogenously expressed FLAG-TLP (data not shown). In contrast, we have detected TLP-dependent luciferase activity driven by pGL3-TAp63-TLP-luc. Indeed, our luciferase reporter construct termed pGL3-TAp63(−487/+26) contained the proximal region and core *TAp63* promoter region, suggesting that there could exist a functional relationship between the proximal and core promoter regions with respect to TLP-dependent transcriptional regulation of *TAp63*. In support of this notion, both TLP and TBP have been shown to be recruited onto *NF1* genomic region containing TLP-responsive element and core promoter sequence (28). Further experiments should be required to adequately address this issue.

Another finding of our present study was that TLP is induced to accumulate in cell nucleus in response to etoposide, and contributes to etoposide-mediated apoptosis through the up-regulation of TAp63. Based on our present results, etoposide treatment promoted the efficient recruitment of the endogenous TLP onto *TAp63* proximal promoter region and resulted in a strong induction of *TAp63* as well as its direct target genes

implicated in apoptosis such as *PUMA*, *NOXA*, and *BAX*. siRNA-mediated knockdown of the endogenous TLP led to a significant down-regulation of TAp63 as well as pro-apoptotic NOXA. Additionally, knocking down of the endogenous TLP resulted in a remarkable inhibition of etoposide-mediated apoptosis as examined by TUNEL assay. Similar results were also obtained in *TAp63*-knocked down cells. In a sharp contrast, Lantner *et al.* found that CD74 stimulation leads to the activation of pro-survival NF-κB and then activated form of NF-κB transactivates TAp63 followed by TAp63-dependent up-regulation of anti-apoptotic Bcl-2 (30). Their observations indicated that NF-κB is one of transcriptional activators for TAp63; however, the up-regulation of TAp63 contributes to cell survival in mature B cells. The differential biological outcomes of the up-regulation of TAp63 might be due to the cellular contexts employed in the experiments. To our knowledge, our present result is a first finding showing that TLP acts as a transcriptional activator for pro-apoptotic TAp63 and participates in the regulation of DNA damage response. Thus, the TLP/TAp63 pro-apoptotic pathway is a novel one in response to DNA damage.

From the clinical point of view, several lines of evidence indicated that the altered expression of *p63* isoforms is observed in human tumor tissues (4), although loss of function mutations in *p63* are rarely detected in various human tumors (6, 7). For example, the dysregulation of the oncogenic *ΔNp63*, which is expressed from a different promoter than that used for expression of *TAp63*, was detectable, especially in squamous cell carcinomas (4, 31). In support with this notion, ΔNp63 contributes to cell survival through a dominant negative effect toward wild-type p53, TAp63, and TAp73 (4, 31). In contrast, the possible involvement of TAp63 in tumor generation might be attributed to its low expression levels in human primary tumors (32, 33). In this connection, higher expression levels of *TAp63* correlated with better prognoses of patients with bladder carcinoma (32). Thus, it is likely that TLP-TAp63 pathway might play an important role in certain tumor suppression. In accordance with this notion, it has been shown that TLP also induces the expression of *NF1*, a representative tumor suppressor gene (20). Given that etoposide stimulates nuclear accumulation of TLP and up-regulation of the *TAp63*, TLP-mediated *TAp63* expression followed by induction of apoptosis might help to suppress tumor generation.

Acknowledgments—We are grateful to Drs. Robert G. Roeder, Jeong H. Park, Tomoe Ichikawa, Miki Ohira, Yohko Nakamura, Hajime Kageyama, Cheng Hong, Kyoung-ae Park, and Tomoko Mabuchi for valuable discussion.

REFERENCES

1. Stiewe, T. (2007) *Nat. Rev. Cancer* **7,** 165–168
2. Yang, A., Kaghad, M., Wang, Y., Gillett, E., Fleming, M. D., Dötsch, V., Andrews, N. C., Caput, D., and McKeon, F. (1998) *Mol. Cell* **2,** 305–316
3. Osada, M., Ohba, M., Kawahara, C., Ishioka, C., Kanamaru, R., Katoh, I., Ikawa, Y., Nimura, Y., Nakagawara, A., Obinata, M., and Ikawa, S. (1998) *Nat. Med.* **4,** 839–843
4. Müller, M., Schleithoff, E. S., Stremmel, W., Melino, G., Krammer, P. H., and Schilling, T. (2006) *Drug Resist. Update* **9,** 288–306
5. Candi, E., Dinsdale, D., Rufini, A., Salomoni, P., Knight, R. A., Mueller, M., Krammer, P. H., and Melino, G. (2007) *Cell Cycle* **6,** 274–285
6. Hagiwara, K., McMenamin, M. G., Miura, K., and Harris, C. C. (1999) *Cancer Res.* **59,** 4165–4169
7. Sunahara, M., Shishikura, T., Takahashi, M., Todo, S., Yamamoto, N., Kimura, H., Kato, S., Ishioka, C., Ikawa, S., Ikawa, Y., and Nakagawara, A. (1999) *Oncogene* **18,** 3761–3765
8. Flores, E. R., Sengupta, S., Miller, J. B., Newman, J. J., Bronson, R., Crowley, D., Yang, A., McKeon, F., and Jacks, T. (2005) *Cancer Cell* **7,** 363–373
9. Flores, E. R., Tsai, K. Y., Crowley, D., Sengupta, S., Yang, A., McKeon, F., and Jacks, T. (2002) *Nature* **416,** 560–564
10. Levrero, M., De Laurenzi, V., Costanzo, A., Gong, J., Wang, J. Y., and Melino, G. (2000) *J. Cell Sci.* **113,** 1661–1670
11. Davidson, I. (2003) *Trends Biochem. Sci.* **28,** 391–398
12. Reina, J. H., and Hernandez, N. (2007) *Genes Dev.* **21,** 2855–2860
13. Ohbayashi, T., Kishimoto, T., Makino, Y., Shimada, M., Nakadai, N., Aoki, T., Kawata, T., Niwa, S., and Tamura, T. (1999) *Biochem. Biophys. Res. Commun.* **255,** 137–142
14. Teichmann, M., Wang, Z., Martinez, E., Tjernberg, A., Zhang, D., Vollmer, F., Chait, B. T., and Roeder, R. G. (1999) *Proc. Natl. Acad. Sci. U.S.A.* **96,** 13720–13725
15. Rabenstein, M. D., Zhou, S., Lis, J. T., and Tjian, R. (1999) *Proc. Natl. Acad. Sci. U.S.A.* **96,** 4791–4796
16. Perletti, L., Dantonel, J. C., and Davidson, I. (1999) *J. Biol. Chem.* **274,** 15301–15304
17. Moore, P. A., Ozer, J., Salunek, M., Jan, G., Zerby, D., Campbell, S., and Lieberman, P. M. (1999) *Mol. Cell. Biol.* **19,** 7610–7620
18. Ohbayashi, T., Shimada, M., Nakadai, T., Wada, T., Handa, H., and Tamura, T. A. (2003) *Nucleic Acids Res.* **31,** 2127–2133
19. Nakadai, T., Shimada, M., Shima, D., Handa, H., and Tamura, T. A. (2004) *J. Biol. Chem.* **279,** 7447–7455
20. Chong, J. A., Moran, M. M., Teichmann, M., Kaczmarek, J. S., Roeder, R., and Clapham, D. E. (2005) *Mol. Cell. Biol.* **25,** 2632–2643
21. Shimada, M., Nakadai, T., and Tamura, T. A. (2003) *Mol. Cell. Biol.* **23,** 4107–4120
22. Ichikawa, T., Suenaga, Y., Koda, T., Ozaki, T., and Nakagawara, A. (2008) *Oncogene* **27,** 409–420
23. Ohbayashi, T., Makino, Y., and Tamura, T. A. (1999) *Nucleic Acids Res.* **27,** 750–755
24. Ozaki, T., and Nakagawara, A. (2005) *Cancer Sci.* **96,** 729–737
25. Gressner, O., Schilling, T., Lorenz, K., Schulze Schleithoff, E., Koch, A., Schulze-Bergkamen, H., Lena, A. M., Candi, E., Terrinoni, A., Catani, M. V., Oren, M., Melino, G., Krammer, P. H., Stremmel, W., and Müller, M. (2005) *EMBO J.* **24,** 2458–2471
26. Petitjean, A., Cavard, C., Shi, H., Tribollet, V., Hainaut, P., and Caron de Fromentel, C. (2005) *Oncogene* **24,** 512–519
27. Park, K. A., Tanaka, Y., Suenaga, Y., and Tamura, T. A. (2006) *Mol. Cells* **22,** 203–209
28. Bush, S. D., Richard, P., and Manley, J. L. (2008) *Mol. Cell. Biol.* **28,** 83–92
29. Martin, D. W., Muñoz, R. M., Subler, M. A., and Deb, S. (1993) *J. Biol. Chem.* **268,** 13062–13067
30. Lantner, F., Starlets, D., Gore, Y., Flaishon, L., Yamit-Hezi, A., Dikstein, R., Leng, L., Bucala, R., Machluf, Y., Oren, M., and Shachar, I. (2007) *Blood* **110,** 4303–4311
31. Rocco, J. W., and Ellisen, L. W. (2006) *Cell Cycle* **5,** 936–940
32. Park, B. J., Lee, S. J., Kim, J. I., Lee, S. J., Lee, C. H., Chang, S. G., Park, J. H., and Chi, S. G. (2000) *Cancer Res.* **60,** 3370–3374
33. Koster, M. I., Lu, S. L., White, L. D., Wang, X. J., and Roop, D. R. (2006) *Cancer Res.* **66,** 3981–3986

nature genetics

FGF9 monomer–dimer equilibrium regulates extracellular matrix affinity and tissue diffusion

Masayo Harada[1,2], Hirotaka Murakami[3,11], Akihiko Okawa[3,11], Noriaki Okimoto[4,11], Shuichi Hiraoka[1,10,11], Taka Nakahara[5,10,11], Ryogo Akasaka[6,11], Yo-ichi Shiraishi[7,11], Noriyuki Futatsugi[4], Yoko Mizutani-Koseki[1], Atsushi Kuroiwa[7], Mikako Shirouzu[6], Shigeyuki Yokoyama[6,8], Makoto Taiji[4], Sachiko Iseki[5], David M Ornitz[9] & Haruhiko Koseki[1]

The spontaneous dominant mouse mutant, Elbow knee synostosis (*Eks*), shows elbow and knee joint synosotsis, and premature fusion of cranial sutures. Here we identify a missense mutation in the *Fgf9* gene that is responsible for the *Eks* mutation. Through investigation of the pathogenic mechanisms of joint and suture synostosis in *Eks* mice, we identify a key molecular mechanism that regulates FGF9 signaling in developing tissues. We show that the *Eks* mutation prevents homodimerization of the FGF9 protein and that monomeric FGF9 binds to heparin with a lower affinity than dimeric FGF9. These biochemical defects result in increased diffusion of the altered FGF9 protein ($FGF9^{Eks}$) through developing tissues, leading to ectopic FGF9 signaling and repression of joint and suture development. We propose a mechanism in which the range of FGF9 signaling in developing tissues is limited by its ability to homodimerize and its affinity for extracellular matrix heparan sulfate proteoglycans.

The fibroblast growth factors (FGFs) are widely expressed in developing and adult tissues and have diverse functions in organogenesis, tissue repair, nervous system control, metabolism and physiological homeostasis[1]. In humans and mice, the 22 FGF ligands are expressed in a spatiotemporally regulated manner and mediate signals through seven different isoforms of FGF receptors (FGFRs)[1]. The pharmacologic potential of FGF ligands has been highlighted by identification of gain-of-function mutations in genes encoding FGFRs 1–3 in individuals with chondrodysplasia and craniosynostosis syndromes[2,3]. These human diseases identify essential roles of FGF signaling not only in development but also in homeostasis of bones and joints.

Given these clinical, genetic and biochemical studies in humans and mice, the coordinated development of bones and joints seems to rely on precise FGFR signaling. This suggests that spatiotemporal constraints on FGF signaling are a prerequisite for appropriate functions *in vivo* and are indeed modulated at several distinct levels. First, the expression of FGF ligands is spatiotemporally restricted. Among the 22 FGF ligands, FGF2, FGF4, FGF7, FGF8, FGF9, FGF10, FGF17 and FGF18 are expressed in the limb bud and developing skeleton[4–6]. Of these, loss-of-function mutations have demonstrated that FGF2, FGF9 and FGF18 are involved in chondrogenesis and/or osteogenesis[7–10]. Induction of chondrodysplastic phenotypes by overexpression of FGF9 in mice also shows its ability to affect chondrogenesis[11]. Other elements implicated in FGF signaling are the heparan sulfate proteoglycans (HSPGs). Genetic studies in mice and *Drosophila melanogaster* suggest that HSPGs regulate the distribution and receptor binding of FGF ligands[12,13]. Finally, structural analyses of FGF9 suggest that it may form homodimers that could affect its ability to signal[14,15]. Because FGF9 homodimerization occludes several critical receptor binding sites, an autoinhibitory mechanism may function to modulate FGF9-dependent signal transduction. However, a functional demonstration of this proposed mechanism is lacking.

We have previously reported that a dominant mouse mutant, Elbow knee synostosis (*Eks*), shows radiohumeral and tibiofemoral synostosis, craniosynostosis (**Supplementary Fig.** 1 online) and lung hypoplasia[16]. In this study, we identify a missense mutation that replaces Asn143 with threonine in the *Fgf9* gene in *Eks* mutant mice. We designate this mutant allele as $Fgf9^{Eks}$ and show that this mutation

[1]RIKEN Research Center for Allergy and Immunology, 1-7-22 Suehiro-cho, Tsurumi-ku, Yokohama, Kanagawa 230-0045, Japan. [2]Department of Immunology and [3]Department of Orthopaedic Surgery, Graduate School of Medicine, Chiba University, 1-8-1 Inohana, Chuo-ku, Chiba 260-8670, Japan. [4]RIKEN Advanced Science Institute, Computational Systems Biology Research Group, 61-1 Ono-cho, Tsurumi-ku, Yokohama, Kanagawa 230-0046, Japan. [5]Section of Molecular Craniofacial Embryology, Graduate School of Medical and Dental Sciences, Tokyo Medical and Dental University, 1-5-45 Yushima, Bunkyo-ku, Tokyo 113-8549, Japan. [6]RIKEN Systems and Structural Biology Center, 1-7-22 Suehiro-cho, Tsurumi-ku, Yokohama, Kanagawa 230-0045, Japan. [7]Division of Biological Science, Graduate School of Science, Nagoya University, Furo-cho, Chikusa-ku, Nagoya 464-8602, Japan. [8]Department of Biophysics and Biochemistry, Graduate School of Science, The University of Tokyo, 7-3-1 Hongo, Bunkyo-ku, Tokyo 113-0033, Japan. [9]Department of Developmental Biology, Washington University School of Medicine, 660 South Euclid Avenue, St. Louis, Missouri 63110, USA. [10]Present addresses: Department of Systems Biomedicine, National Research Institute for Child Health and Development, 2-10-1 Okura, Setagaya-ku, Tokyo 157-8535, Japan (S.H.) and Section of Developmental and Regenerative Dentistry, School of Life Dentistry at Tokyo, The Nippon Dental University, 1-9-20 Fujimi, Chiyoda-ku, Tokyo 102-8159, Japan (T.N.). [11]These authors contributed equally to this work. Correspondence should be addressed to H.K. (koseki@rcai.riken.jp).

Received 20 June 2008; accepted 22 December 2008; published online 15 February 2009; doi:10.1038/ng.316